

THESIS FOR THE DEGREE OF DOCTOR OF PHILOSOPHY

Applicable Directivity Description of Railway Noise Sources

XUETAO ZHANG

Department of Civil and Environmental Engineering
Division of Applied Acoustics, Vibroacoustic Group
CHALMERS UNIVERSITY OF TECHNOLOGY
Göteborg, Sweden 2010

Applicable Directivity Description of Railway Noise Sources

XUETAO ZHANG

ISBN 978-91-7385-416-0

© Xuetao Zhang, 2010

Doktorsavhandlingar vid Chalmers tekniska högskola

Ny serie nr 3097

ISSN 0346-718X

Department of Civil and Environmental Engineering

Division of Applied Acoustics

Chalmers University of Technology

SE – 412 96 Göteborg

Sweden

Tel: +46 (0) 31-772 2200

Fax: +46 (0) 31-772 2212

Cover:

3D directivity pattern of a perpendicular dipole pair, viewed along the axis of the red dipole component which is 4 dB weaker than the blue one.

Printed by

Chalmers Reproservice

Göteborg, Sweden, 2010

Applicable Directivity Description of Railway Noise Sources

XUETAO ZHANG

Department of Civil and Environmental Engineering

Division of Applied Acoustics

Chalmers University of Technology

Abstract

For a sound source, directivity is an important parameter to specify. This parameter also reflects the physical feature of the sound generation mechanism. For example, turbulence sound is of quadrupole directivity while fluid-structure interaction often produces a sound of dipole characteristic. Therefore, to reach a proper directivity description is in fact a process of understanding the sound source in a better way. However, in practice, this is often not a simple procedure. As for railway noise engineering, several noise types of different directivity characters are often mixed together, such as wheel and rail radiation, engine and cooling fan noise, scattered fluid sound around bogies and turbulent boundary layer noise along train side surfaces. Moreover, it is a question if the horizontal directivity of a line source can be measured directly. All these factors increase difficulties to reach a proper directivity description that may explain why modelling directivities of railway noise sources is so far behind modelling their sound powers.

This thesis work aims at working out an applicable directivity description of railway noise sources. The study focuses on the two most important railway noise types, i.e. rolling noise and aerodynamic noise. Directivities of these two noise types are studied based on measurement investigation, theoretical problem solution and model analysis. As for rolling noise, a model of *perpendicular dipole pair* (PDP) is proposed to interpret those measurement specified directivity characteristics of wheel/rail radiation. This model naturally explains why a vibrating railway wheel does not present dipole directivity and why rail radiation is of different horizontal and vertical directivities. As for aerodynamic noise, it has been found that pantograph noise is also of perpendicular dipole components. Moreover, for aerodynamic noise around bogies, *scattering* of the air flow is proposed to be the dominant mechanism of the noise generation. This understanding leads to a different directivity description for this noise component. And, once again, scattered fluid sound around bogies and turbulent boundary layer noise along train side surfaces can be treated as a PDP source. Finally, to complete directivity description of railway noise, directivities of other important noise types have been studied as well; the directivity characteristics of these noise types become understood although lack the relevant directivity data. With all these outputs integrated, a survey of the directivities of all important railway noise sources has been achieved and applicable directivity functions have been worked out. Hopefully, this directivity study provides values not only for railway noise engineering but also for a better understanding of railway noise.

Key words railway noise; directivity; perpendicular dipole pair; scattered fluid sound; the Doppler factor

Thesis publications

The thesis consists of the work presented in the following appended papers:

Paper I

X. Zhang, To determine the horizontal directivity of train pass-by noise, in03_627, *The Proceedings of inter.noise03*, 25-28 August, 2003, Jeju, Korea.

Paper II

X. Zhang and H. Jonasson, Directivity of Railway Noise Sources, *Journal of Sound and Vibration* 293 (2006) 995–1006.

Paper III

X. Zhang, Directivity of Railway Rolling Noise, Noise and Vibration Mitigation for Rail Transportation Systems, *Notes on Numerical Fluid Mechanics and Multidisciplinary Design*, Volume 99, ©2008 Springer-Verlag Berlin Heidelberg.

Paper IV

X. Zhang, Modelling the directivity of wheel/rail vibration noise using a circular/straight line of perpendicular dipole pairs, *The 10th International Workshop on Railway Noise*, IWRN10, 18-22 October, 2010, Nagahama, Japan.

Paper V

X. Zhang, The Directivity of Railway Noise at Different Speeds (accepted by *Journal of Sound and Vibration*).

My contribution in paper 2 is estimated at about 90 %.

The related works which are not included in this thesis:

X. Zhang, Diesel locomotive noise - An example of source localization, HAR12MO-020220-SP04.

X. Zhang, Railway Traction Noise – the state of the art, HAR12TR-030530-SP01.

X. Zhang, Measurements of Directivity on Test Rig, HAR12TR-020910-SP04, 30 April, 2003.

X. Zhang, The formulation of sound-power allocation of railway noise sources, IMA6MO-040830-SP04, 2004-09-24.

X. Zhang, On the Directivity of Railway Noise Sources, the licentiate dissertation, lic 2007:3, ISSN 1652-9146, Chalmers University of Technology.

ACKNOWLEDGEMENTS

I began my career in acoustics exactly when I started at SP Acoustics in 1999. Docent Dr. Hans G. Jonasson, who at that time was the head of the Acoustics Section, introduced me to modelling traffic noise with the focus on railway noise - an interesting research field. It is during the European project Harmonoise that I started to investigate directivities of railway rolling noise and traction noise. SP's directivity measurement campaign, which is carried out by me but designed and arranged by Hans, provides valuable information on the directivities, and also serves as a solid foundation for the further study on the problem. It is no exaggeration to say that the directivity study would not be successful if these directivity measurements had not been proposed.

I am also grateful to Prof. Wolfgang Kropp, who is the head of the Division of Applied Acoustics at Chalmers, not only for him to provide me the post of Ph.D. study but also for his insistence on the importance of academic value, that pushes me and drives me to reach a balance between practically handling and theoretically modelling in the thesis work.

I feel greatly indebted to my third supervisor Dr. Krister Larsson, who is the current head of SP Acoustics. Krister supports me in various aspects during the second phase of the study, which provides me with a comfort platform to complete the thesis project. I really appreciate this platform and would like to continue my research life with it.

Taking this opportunity I would like to thank two of my colleagues at SP Acoustics, Håkan Andersson and Mohammad Jalalian, who helped me to carry out various directivity measurements at the Railway Noise Test Rig in Surahammar, in the field or in the SP lab.

I would also like to thank Ms Gunilla Skog and Mr Börje Wijk for helping me with many routine issues in the Division of Applied Acoustics. Thanks also to all the colleagues in the Division for keeping a warm and active research atmosphere.

Finally, I would like to give my heartfelt thanks to my wife Jie and my daughter Yiting for a lovely atmosphere at home which is the pivotal support to my research life.

Xuetao Zhang
SP Acoustics, Borås, April 2010

Contents

| | | |
|---------------------------|--|-----------|
| 1 | Background and Aim | 1 |
| 1.1 | Research on railway noise..... | 1 |
| 1.2 | Directivity of railway noise..... | 4 |
| 1.3 | The aim of the thesis | 5 |
| 1.4 | The structure of the thesis | 5 |
| 1.5 | Overview of the appended papers | 6 |
| 2 | SP's Directivity Measurement Campaign | 9 |
| 2.1 | Measuring directivity of wheel/rail radiation | 9 |
| 2.2 | Measuring vertical directivity of train pass-by noise..... | 13 |
| 2.3 | Measured directivity of wheel radiation reported by other researchers | 15 |
| 2.4 | Some discussion | 19 |
| 2.5 | Measurement of locomotive noise | 19 |
| 3 | Directivity Description of Railway Noise | 25 |
| 3.1 | Rolling noise..... | 25 |
| 3.2 | Aerodynamic noise..... | 31 |
| 3.3 | Other important noise types | 37 |
| 4 | Conclusions and Future Works | 39 |
| Annex A | Calculation Procedure to Determine the Equivalent Horizontal Directivity of A Line Source | 41 |
| Annex B | Calculation of Aerodynamic Noise | 51 |
| Bibliography | | 55 |

1 Background and Aim

1.1 Research on railway noise

Nowadays, our achievements in modern science and technology provide us with the power not only to understand the nature of the world around us but also to exploit natural resources for our various needs. However, we have also begun to realize that many improper applications of modern technology have had serious harmful impacts on our natural environment. A list of such impacts is quite long, e.g. different kinds of pollution (air, water, waste, noise ...) and an increasing scarcity of resources (water, oil ...). Thus, it now becomes an important issue for us to consider how to apply modern techniques properly and in an integrated manner in order to obtain the most benefits from them but meanwhile to reduce harmful side effects to the least extent. In other words, a sustainable development of eco-solutions is desired.

Three-dimensional modern transportation, i.e. on-land (and underground), cross-water and in-air transportation, provides us with great mobility which is one key parameter that a modern society should possess. However, it has two major negative impacts on our environment: traffic noise and air pollution. Traffic noise is the most serious outdoor noise source which, together with other influencing noise types including industrial noise, construction noise, entertainment noise and residential noise, has caused our acoustical environment to frequently fall short of WHO recommendations [1]. As has been reported, more than 100 million (about one eighth) Europeans are exposed to outdoor equivalent noise levels above 65 dB ($L_{Aeq,24h}$), which scientists and health experts consider unacceptable. Unquestionably, we need to work hard to improve our acoustical environment.

Railway transportation is an environmentally friendly transportation mode except for its noise impact. (When diesel locomotive traction is relevant air pollution, although quite limited, is also a concern.) "... the problem of noise from road, rail and air transport is identified as one of the most urgent areas for action" [2]. "It is estimated that more than 30 % percent of Europeans are exposed to road noise levels, and around 10 % to rail noise levels, above 55 L_{dn} dB(A)" [3]. Accordingly, rail vehicles have been identified as one of the major noise sources.

In the past four decades, extensive research on railway noise has been carried out in order to understand the noise generation mechanisms of its different sub-sources and to invent various means to reduce the noise levels [4]. As for rolling noise, especially, Remington and his group set up the preliminary models [5-9] and Thompson made major further developments [10]. In 1991 Thompson's prediction model was

implemented into the calculation software TWINS (Track-Wheel Interaction Noise Software) [11, 12]. The TWINS has proved to be a powerful tool for studying rolling noise and various related noise reduction concepts. Moreover, many following EU-founded research projects contribute not only to understanding railway noise but to developing techniques for reducing railway noise at source. I would like to mention those projects: MetaRail, STAIRRS, Silent Freight, Silent Track, Eurosabot, NOEMIE, Harmonoise and Imagine [13-18]. Thanks to all the achievements since the 1970s, it has now become well understood how to control railway noise - as the slogan of the IPG final international seminar declared: “Farewell symptoms, hello innovation solutions” [19].

Table 1.1 Countries with modern high speed trains [21-28]

| Country | High Speed Train | Top Service Speed (km/h) | Note |
|---------------|------------------|--------------------------|--|
| Japan | Shinkansen | 300 | Inaugural service was on 1 October, 1964. The first Shinkansen trains ran 210 km/h. Earthquake warning system and anti-derailment device are two advanced technology. Fastech 360 test trains are currently not feasible. |
| France | TGV | 320 | LN 1, inaugural service was on 22 September, 1981; LN 2, 1989; LN 3, 1993; LN 4, 1992; LN 5, 2001; LGV Est, 2007. HSL based on LGV technology connecting with the French network have also been built in Belgium, the Netherlands and UK. Record speed 574,8 km/h on 3 April, 2007 |
| Germany | ICE | 320 | ICE 1, inaugural service was on 29 May, 1991; ICE 2, 1996; ICE T & ICE 3, 1999; ICE TD, 2001-2003, back 2007. ICE 3 is built as EMU. Made by a consortium of Bombardier and Siemens. ICE variations are also found in Spain, China and Russia. |
| Italy | ETR 500 | 300 | Italy was a pioneer in rail travel in the 1930s. Prototype set ETR 500-X in 1994. |
| Spain | AVE | 300 | Inaugural service was on 21 April, 1992. Velaro trains are based on ICE 3. |
| Korea | KTX | 300 | Inaugural service was on 1 April, 2004. Largely based on French TGV/LGV system. HEMU-400X with 400 km/h top speed will be possible by 2012 |
| China | CRH | 350 | Inaugural service was on 1 August, 2008. CRH1 is based on Bombardier's Regina; CRH2 is a modified E2-1000 series Shinkansen; CRH3 is based on Siemens' Velaro; CRH5 is based on Alstom Pendolino ETR-600. |
| China, Taiwan | THSR | 300 | Inaugural service was on 2 March, 2007. Based on Shinkansen 700 Series. |

However, the requirement is high - it is likely that a further noise reduction of 10-15 dB(A) in exposure “is necessary across Europe to provide significant improvement in noise exposure levels for the majority of the population affected by railway noise” [20].

High-speed rail transportation is developing apace. After the first modern high-speed line, the Japanese Shinkansen line which inaugurated its services on October 1st, 1964, France and Germany have built up their high speed rail systems. More and more high speed trains are appearing on lines in Europe and recently also in Asia; a main line of the development is summarized in table 1.1 [21-28]. Since the beginning of 21st century, construction of high-speed rail lines is under acceleration, especially from 2008 when China began to build up her high-speed rail network of about 13,000 km in total length. It seems that a wave of construction of high-speed rail lines is to be triggered on. For example, EU Trans-European high-speed rail network is going to link not only the north and the south but also the west and the east. In Asia, an East-South Asian high-speed rail line linking the south of China and Singapore is under consideration. In America, USA, Brazil and Venezuela are to build up their high-speed rail lines. Moreover, the UK is now discussing building up a high-speed rail line linking Scotland and London, with a top service speed of 400 km/h. These plans of world-scale investment on high-speed rail networks, which may imply a transport revolution in the 21st century, will have a profound influence on our daily lives.

With the development of high-speed rail transportation, railway aerodynamic noise becomes more of a concern and systematic researches on this noise type have been carried out since the early 1990s; such research in Europe is mainly within the frame work of German-French cooperation [4]. With these researches, which are mainly based on microphone array investigations while also including some wind tunnel studies and numerical simulations, understanding of this noise type is improved [4, 29-37]. Briefly, it has been learnt that important aerodynamic noise sources are scattered fluid sound around the bogies, vortex shedding from the pantograph and wake eddies at the train rear, while turbulence noise, radiated from the inter-coach areas of a train, contributes much less.

In the past, railway traction noise could be important even up to 200 km/h [38], while today it is a dominant noise type only at low speed. For modern traction units, locomotives, DMUs, EMUs and DEMUs¹, the dominant noise sources are cooling fans and traction engine/motor(s). Fan noise is still an active research topic. While, as for engine noise, although there is no a general method to predict its sound power level, “the foundation of the present understanding of noise generation by the combustion process was established by Austen and Priede between 1958 and 1966 and much further work has been done since then by other investigators ” [38]. Presently, the main effort on reducing traction noise is to apply various measures of vibration isolation, sound absorption and sound insulation.

There are other noise types which are important under different operating conditions. These noise types include brake noise, impact sound, curve squeal and bridge noise.

¹ A Diesel or Electric or Diesel Electric Multiple Unit is a self-propelling train unit capable of coupling with other units of the same or similar type and still being controlled from one cab.

The nature of these noise types has been understood [4], while, for most of them, quantitative predictions of their sound powers are still not available.

1.2 Directivity of railway noise

For a sound source, directivity is an important parameter to specify. This parameter also reflects the physical feature of the sound generation mechanism. For example, turbulence sound is of quadrupole directivity while fluid-structure interaction often produces a sound of dipole characteristic. Therefore, to reach a proper directivity description of a sound source is in fact a process of understanding it better. However, this is often not a simple procedure. In railway noise engineering, several noise types of different directivity characters are often mixed together, such as wheel and rail radiation, engine and cooling fan noise, scattered fluid sound around the bogies and turbulent boundary layer noise along train side surfaces. Moreover, it is a question if horizontal directivity of a line source can be measured directly. All these factors increase the difficulty of making a proper directivity description, and may explain why modelling directivities of railway noise sources is far behind modelling their sound powers.

Over the past four decades, many measurement studies on the directivity of rolling noise have been carried out [5, 39-50]. However, these directivity studies focus on different noise components or operating conditions; the measured directivity data are also greatly dependent on the measurement setups. Understanding of the directivity of rolling noise is not unified; some directivity measurements are even improperly interpreted, as directivity pattern of a sound source can be distorted by a number of factors such as interference between component sound rays, ground reflection and absorption, the shielding and/or reflection and/or diffraction of nearby constructions together with the radiation of the vibrating foundations, and the effect of source dimension. Therefore, it would be advantageous to inspect these measurement studies systematically in order to achieve a directivity description which is not only properly understood but also useful for engineering applications.

During the European project Harmonoise, a preliminary directivity estimation for various aerodynamic sources was proposed [30], as summarized in the following: (1) one set of directivity data of pantograph noise is provided in tabular values, which shows dipole directivity character in the horizontal direction (this directivity character has been proved in Paper V) and is slightly directional in the vertical direction (about 4 dB higher in sound power level in the vertical direction than in the lateral direction); (2) inter-coach noise is less directional than aerodynamic sound around bogies; (3) due to a lack of information about their directivity, all sub-sources except pantograph noise are assigned the same directivity which is given by

$$5 * \ln[\sin(\varphi + \pi/2)], \quad (1-1)$$

where the horizontal angle, φ , is defined as shown in Fig. 1.1.

As has been pointed out in Paper V, the directivity given by Eq. (1-1) is in fact the one for turbulent boundary layer noise; aerodynamic noise around bogies is of a

different directivity. Since the latter is a predominant component, the Harmonoise proposal for the directivity of aerodynamic noise needs to be revised.

Quite a few measurement studies on the directivity of traction noise have been reported [51-52]. For other important noise types, i.e. impact sound, curve squeal, brake noise and bridge vibration noise, no measurement or other kind of studies on the directivities can be found in literature. Therefore, investigation on the directivities of these noise types is needed.

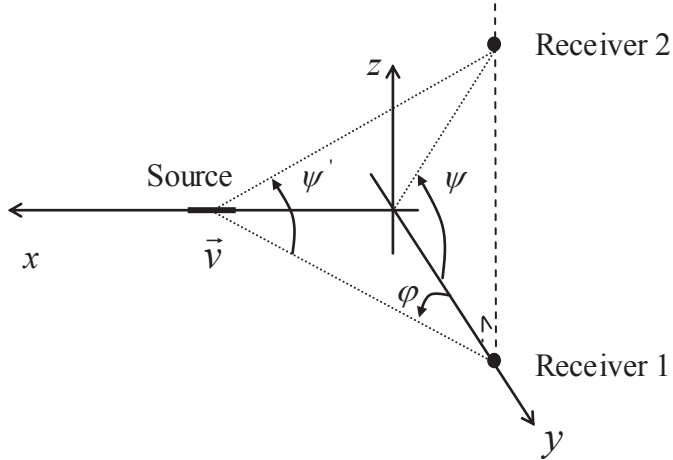


Fig. 1.1. The definition of angles: φ is a horizontal angle in the x - y plane and relative to the y -axis; ψ is a vertical angle in the y - z plane; ψ' is a vertical angle in a vertical plane containing the receiver and the source (or the centre of the source line).

1.3 The aim of the thesis

The aim of this thesis project is to work out a directivity description of railway noise, which should both be based on proper understanding and be applicable for railway noise engineering.

Considering that many sub-sources are involved while not all directivity data are available, the study focuses on the two most important noise types, i.e. rolling noise and aerodynamic noise. Directivities of other important noise types have been studied as well while focusing on understanding their directivity characteristics. In this way, the directivity study is made complete and a survey of the directivities of all important railway noise sources has been achieved.

1.4 The structure of the thesis

First, in chapter 2, SP's measurement campaign on directivities of rolling noise and traction noise will be described. Moreover, through comparing the directivity measurements made by other researchers, special issues concerned with directivity measurement will be discussed. Next, in chapter 3, directivities of railway rolling

noise, aerodynamic noise and other important noise types, together with the treatment at high speed will be discussed in the relevant sections under the chapter based on the work presented in appended papers. Thereafter, in the last chapter, conclusions will be made and future works will be proposed.

1.5 Overview of the appended papers

Paper I: In this paper, a calculation procedure is proposed to determine the equivalent horizontal directivity of a line of incoherent point sources, aiming at determining the horizontal directivity of train pass-by noise. With this calculation procedure, (1) the horizontal directivity of rail radiation which cannot be measured directly can be verified by applying the directivity data of wheel radiation and the one of the total rolling noise at a distance; (2) the effect of source dimension on the horizontal directivity can be handled properly.

The discussion of this issue is re-formulated and presented in Annex A, with some practical examples provided.

Paper II: In this paper, the first attempt is made to propose the directivity of railway noise. Directivities of rolling noise and its components, wheel and rail radiation, are discussed in detail based on SP's directivity measurements and the data analyses, together with available literature on relevant directivity measurements. However, directivities of traction noise and aerodynamic noise are handled only qualitatively due to a lack of relevant directivity data. As can be seen, this first proposal is in a preliminary phase. The improvements are made in the following papers.

Paper III: Directivities of rolling noise including its components, i.e. wheel and rail radiation, are studied systematically. The directivity characteristics of the noise type become well understood. And, applicable directivity functions in one-third octave bands or, a calculation procedure to determine the directivity function, are proposed. What is missing in the paper is how to handle the effect of high speed motion.

Paper IV: In this paper a model is proposed to interpret the directivity characteristics of wheel/rail radiation. With the proposed model of *perpendicular dipole pair* for rail and wheel radiation, the measurement specified horizontal and vertical directivities can naturally be explained. This model provides a novel and promising understanding of the physical feature of railway rolling noise.

Paper V: This paper may be considered as the final proposal for describing directivity of railway noise, although the details of the directivity description given in this paper could be subjected to some revisions in future. In this paper, a comprehensive study on the directivities of all important railway noise sources is presented. First, as for rolling noise, the measurement specified directivities presented in paper III and the model description presented in paper IV are harmonically combined together; and, the handling of high speed motion is added. Next, as for aerodynamic noise, one set of directivity data of pantograph noise provided by SNCF (Société Nationale des Chemins de fer Français, French National Railways) is analysed and it has been found that the pantograph noise is also of perpendicular dipole components! Moreover, for the most important component of aerodynamic sound - aerodynamic sound around

bogies, *scattering* of the air flow is proposed to be the dominant mechanism of the noise generation. This distinct understanding leads to a directivity description different from what has previously been proposed. Third, as for other important noise types which include traction noise, impact sound, curve squeal, brake noise and bridge noise, relevant directivities are studied as well. The directivity characteristics of these noise types become understood although lack the relevant directivity data. With all these outputs integrated, the directivity study is made complete and a survey of the directivities of all important railway noise sources has been achieved.

2 SP's Directivity Measurement Campaign

2.1 Measuring directivity of wheel/rail radiation

As part of the Harmonoise project, SP Acoustics launched a measurement campaign to investigate directivities of wheel radiation, rail radiation and train pass-by noise.

SP Acoustics has an informal cooperation with CHARMEC [53], Competence Centre in Railway Mechanics established at Chalmers University of Technology (CHAlmers Railway MEchanics). There are three parties involved in CHARMEC: the Industrial Interests Group, Chalmers University of Technology and the Swedish Agency for Innovation Systems (VINNOVA). Lucchini Sweden, a Lucchini subsidiary and wheelset manufacturer located in Surahammar, is a member of the Industrial Interests Group. Via this informal cooperation, SP Acoustics has been offered the opportunity to use the Railway Noise Test Rig (RNTR) at Lucchini Sweden (Fig. 2.1).



Fig. 2.1. The Railway Noise Test Rig at Lucchini Sweden in Surahammar

With the help of a robotic positioning system, a microphone is able to scan over the fictitious surface of about a quarter sphere of radius 2.45 m, as shown in Fig. 2.1. Dynamic contact forces between wheel and rail are simulated by applying force

actuators acting on the wheel or rail, in a vertical and/or lateral direction (Fig. 2.2). When measuring directivity of wheel radiation, the sampling grid shown in Fig. 2.3 is used which is defined in table 2.1. Moreover, a reference microphone is placed close to angle position $(0^\circ, 0^\circ)$ as shown in Fig. 2.4(a); the recording of this microphone is used to calibrate the sound pressure levels sampled at each grid point.



Fig. 2.2. The vertical and lateral force actuators

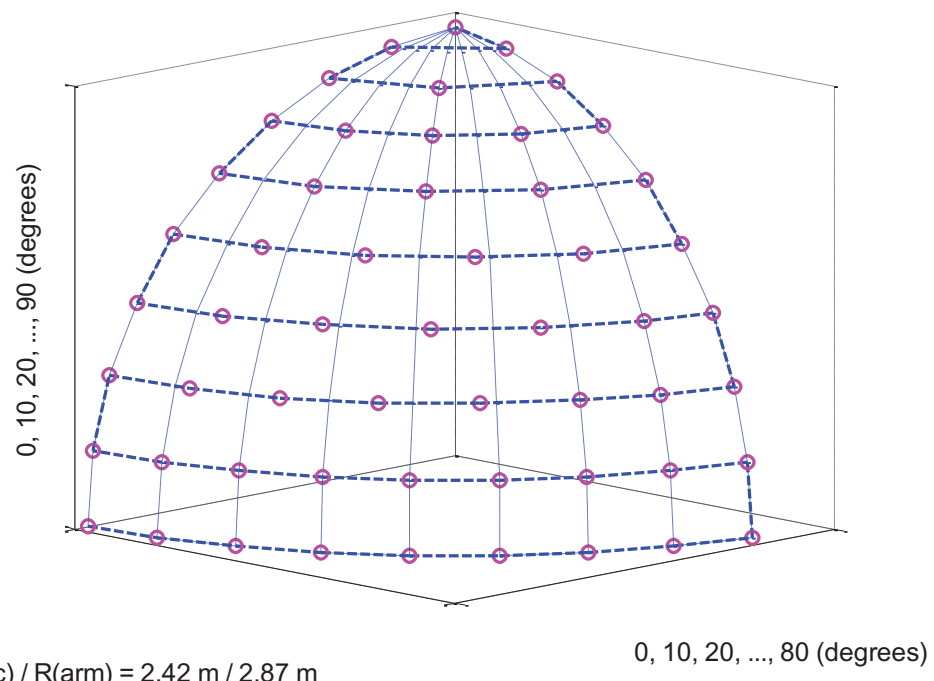
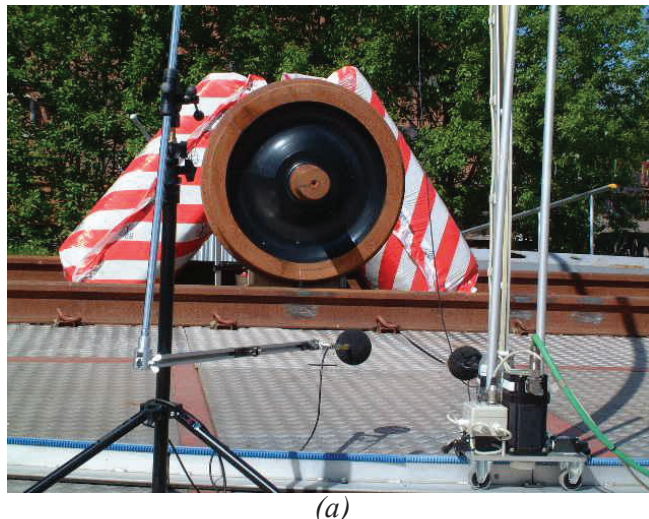


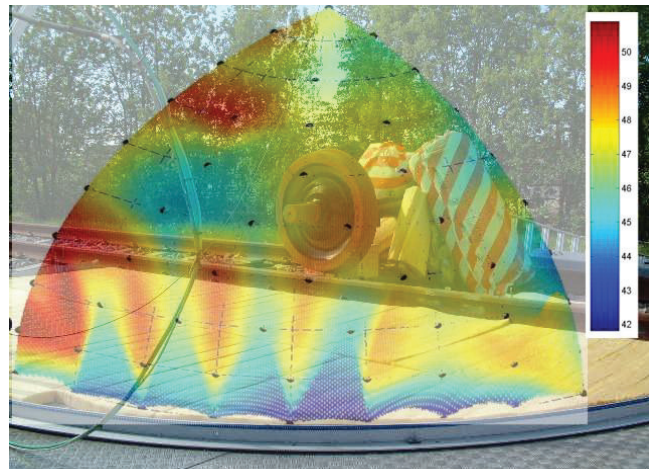
Fig. 2.3. The sampling grid which is on a fictitious surface of a quarter sphere of radius 2.45m and is made for measuring directivity of wheel radiation; see also Fig. 2.4(b).

Table 2.1 The SP sampling grid for measuring directivity of wheel radiation

| Vertical angle (degree) | Horizontal angle (degree) | | | | | | | | |
|----------------------------|------------------------------|----|----|----|----|----|----|----|----|
| | 0 | 10 | 20 | 30 | 40 | 50 | 60 | 70 | 80 |
| 0 | 0 | 10 | 20 | 30 | 40 | 50 | 60 | 70 | 80 |
| 10 | 0 | 10 | 20 | 30 | 40 | 50 | 60 | 70 | 80 |
| 20 | 0 | 12 | 24 | 36 | 48 | 60 | 70 | 80 | |
| 30 | 0 | 14 | 28 | 42 | 56 | 70 | 80 | | |
| 40 | 0 | 16 | 32 | 48 | 64 | 80 | | | |
| 50 | 0 | 20 | 40 | 60 | 80 | | | | |
| 60 | 0 | 20 | 40 | 60 | 80 | | | | |
| 70 | 0 | 40 | 80 | | | | | | |
| 80 | 0 | 80 | | | | | | | |
| 90 | 0 | | | | | | | | |



(a)



(b)

Fig. 2.4. Measuring directivity of wheel radiation at RNTR in Surahammar. (a) The wheelset, reference (left) and sampling microphones; (b) the recorded SPLs on the fictitious surface of a quarter sphere (the level differences are within about 5 dB).

A standard freight car wheelset SJ 57H is used. The measured directivity of wheel radiation has been analysed [40] and presented in Fig. 2.4(b), and discussed in all appended papers. Moreover, the directivity of wheel radiation of the same wheelset is measured again about two years later in SP's semi-anechoic chamber. Taking this second opportunity, the directivity has been re-inspected by measuring the spatial distribution of the wheel radiation with alleviated ground reflection (by placing 40 cm thick mineral wool on the ground, see Fig. 2.5). A similar directivity pattern is obtained.

At the RNTR in Surahammar, vertical directivity of rail radiation has also been measured, see Fig. 2.6.



Fig. 2.5. Measuring horizontal or vertical directivity of wheel radiation in SP's semi-anechoic chamber with the ground covered by 40 cm thick mineral wool



Fig. 2.6. Measuring vertical directivity of rail radiation at the RNTR in Surahammar

To investigate the shielding effect of the car body on vertical directivity of rolling noise, a simplified construction is made and put above the wheelset, as shown in Fig. 2.7(a). In approximate terms, this simplified construction is, in its shielding effect,

close to that of the car bodies shown in Fig. 2.7(b). This measurement provides the information on the shielding effect for the type of car bodies. However, the data cannot be used to other train types and near track barriers (Fig. 2.8) because the shielding effects of them on vertical directivity of rolling noise may be very different.

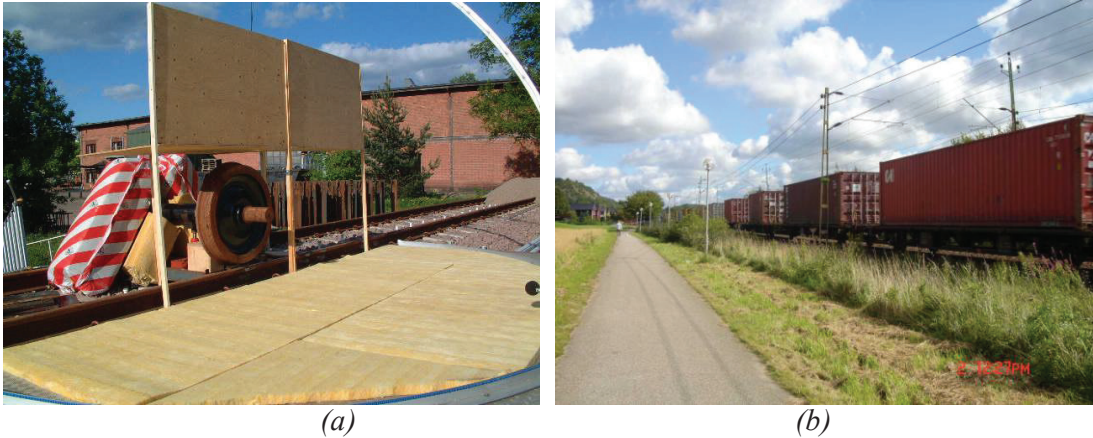


Fig. 2.7. (a) Measuring shielding effect of “car body” on vertical directivity of wheel radiation; (b) the type of car body which is simulated by the simple structure shown in (a).

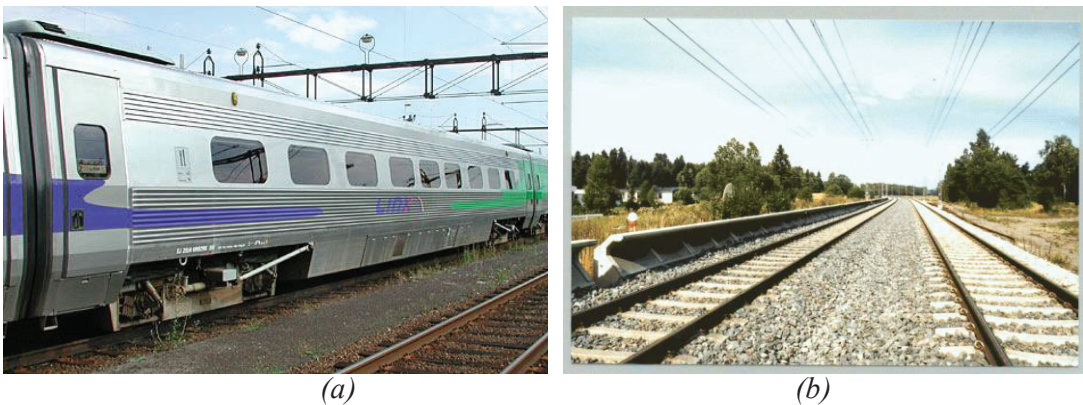


Fig. 2.8. (a) The car body of an X2000 train; (b) a near track low barrier

2.2 Measuring vertical directivity of train pass-by noise

Way-side vertical directivity of train pass-by noise is investigated at Sandared – Viken in Borås where the railway track bed is about 2.9 m above the ground (Fig. 2.9). Therefore, if taking the rail top height (about 3.05 m above the ground) as the reference, ground effect on the train noise recorded at this height has no major difference compared to that recorded at higher positions. In other words, at this site, the vertical directivity data recorded at vertical angle positions between 0° and 45° contain similar ground effect.

The measured vertical directivity data are presented in Fig. 2.10. It can be seen that, if taking away the recordings at the two lowest positions where the strong ground effect is present, way-side vertical directivity of the train pass-by noise is not important.



(a) Measurement setup



(b) X11 train

Fig. 2.9. Measuring vertical directivity of train pass-by noise by eight microphones located at respective angle positions of -14.8° , -7.7° , 0° , 5.1° , 19.9° , 26.8° , 33° and 38.6° . The respective microphone heights relative to the rail top are: -2.80, -1.50, 0, 1, 3.53, 4.94, 6.35 and 7.80 (m). (a) The two microphone stands, of which each has four microphones mounted on. (b) An X11 train was passing by.

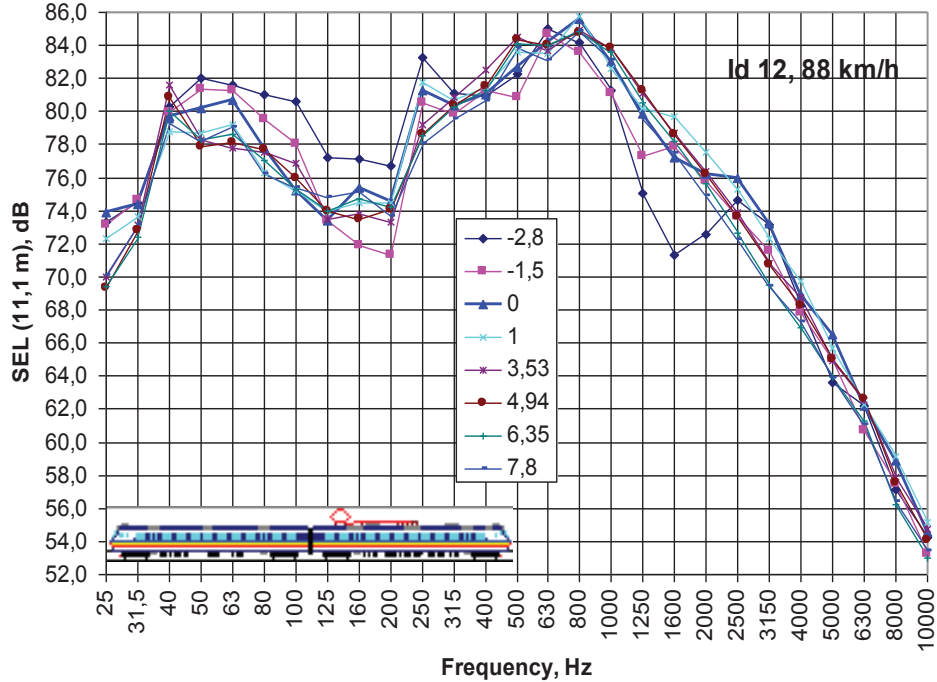


Fig. 2.10. Normalized SEL-levels of an X11 train passing-by at 88 km/h, recorded at the eight heights.

2.3 Measured directivity of wheel radiation reported by other researchers

Since a directivity measurement can be affected by a number of factors such as measurement setup or ground reflection and absorption, it is helpful to refer to related measurements made by others. In literature, except SP's report, one can find a few reports on measuring directivity of wheel radiation: one by Remington [5] and another by Thompson [4]. Moreover, Wolde and Ruiten also reported that their directivity data of wheel radiation were different from what Remington reported [47]; however, they did not present their directivity data to the public.

Remington's wheel directivity data is shown in Fig. 2.11 and the one reported by Thompson is shown in Fig. 2.12. The wheel directivity measured by SP is presented in Fig. 2.13. By comparison one can clearly see that all directivity data contain interference effect: in the data reported by Thompson and the ones measured by SP interference effects are very strong, while interference effects in Remington's data are not strong. In other words, Remington's wheel directivity data in one-third octave bands clearly show the directivity pattern, which is supported by SP's wheel directivity data in total A-weighted SPL (Fig. 2.13(a)). The possible reason that Remington's data contain less interference effects has been discussed in Paper III.

Due to the strong interference effects contained in SP's wheel directivity data in one-third octave bands (Fig. 2.13, (b) ~ (f)), it is in fact difficult to draw a conclusion on the directivity. What has been tried is to use the “envelop” of a directivity curve to define the directivity pattern, as constructive interference will at maximum raise the

level by 6 dB while destructive interference can reduce the level by any extent. Also assumed in the analysis is that directivity patterns between neighbour (one-third octave) bands shall not differ much (when the interference effect has been removed). In this way, the directivity pattern is obtained for the one-third octave bands data, which is roughly the same as that for the total A-weighted SPL.

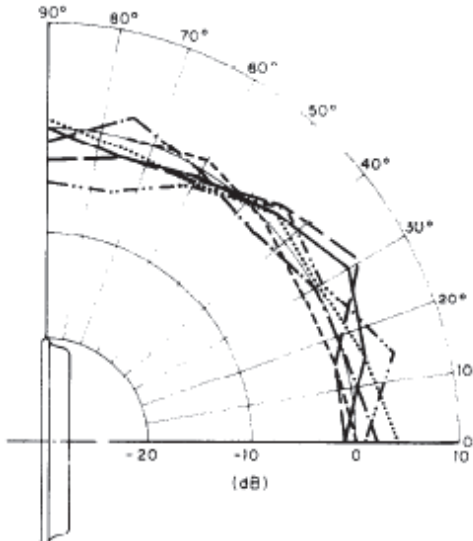


Figure 14. One-third-octave band wheel directivity under axial forcing. —, 4 kHz; -·-, 3 kHz;
—·—, 2 kHz; ——, 1 kHz; ·····, 630 Hz; -·—, 315 Hz.

(a)

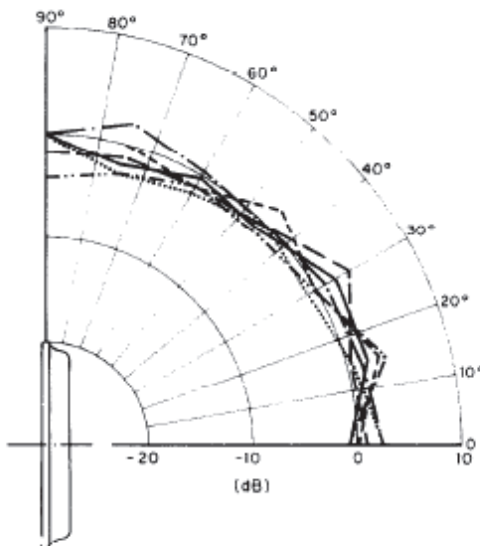


Figure 15. One-third-octave band wheel directivity under radial forcing. —, 4 kHz; -·-, 3 kHz;
—·—, 2 kHz; ——, 1 kHz; ·····, 630 Hz; -·—, 315 Hz.

(b)

Fig. 2.11. The directivity of wheel radiation reported by Remington [5]. (a) Under axial excitation. (b) Under radial excitation.

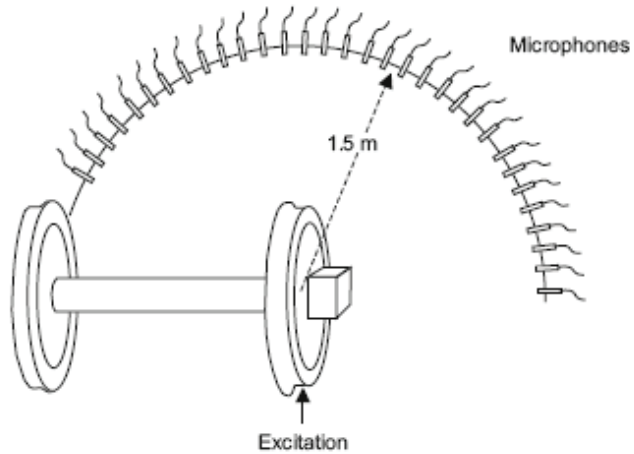


FIGURE 6-11 Location of microphones around a wheel to measure directivity

(a)

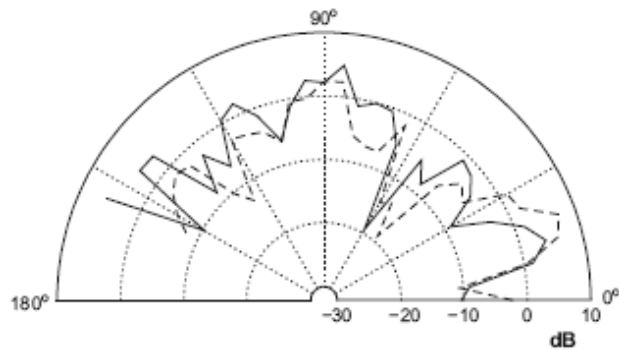


FIGURE 6-12 Directivity of an NS Intercity wheel for radial modes. The wheel axis lies at the angle 0° , angles greater than 90° represent positions behind the wheel. —, $n = 3, 2470\text{ Hz}$; ---, $n = 5, 4060\text{ Hz}$, adapted from [6.14]

(b)

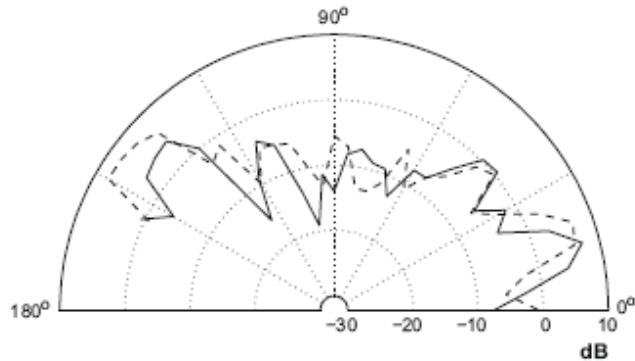
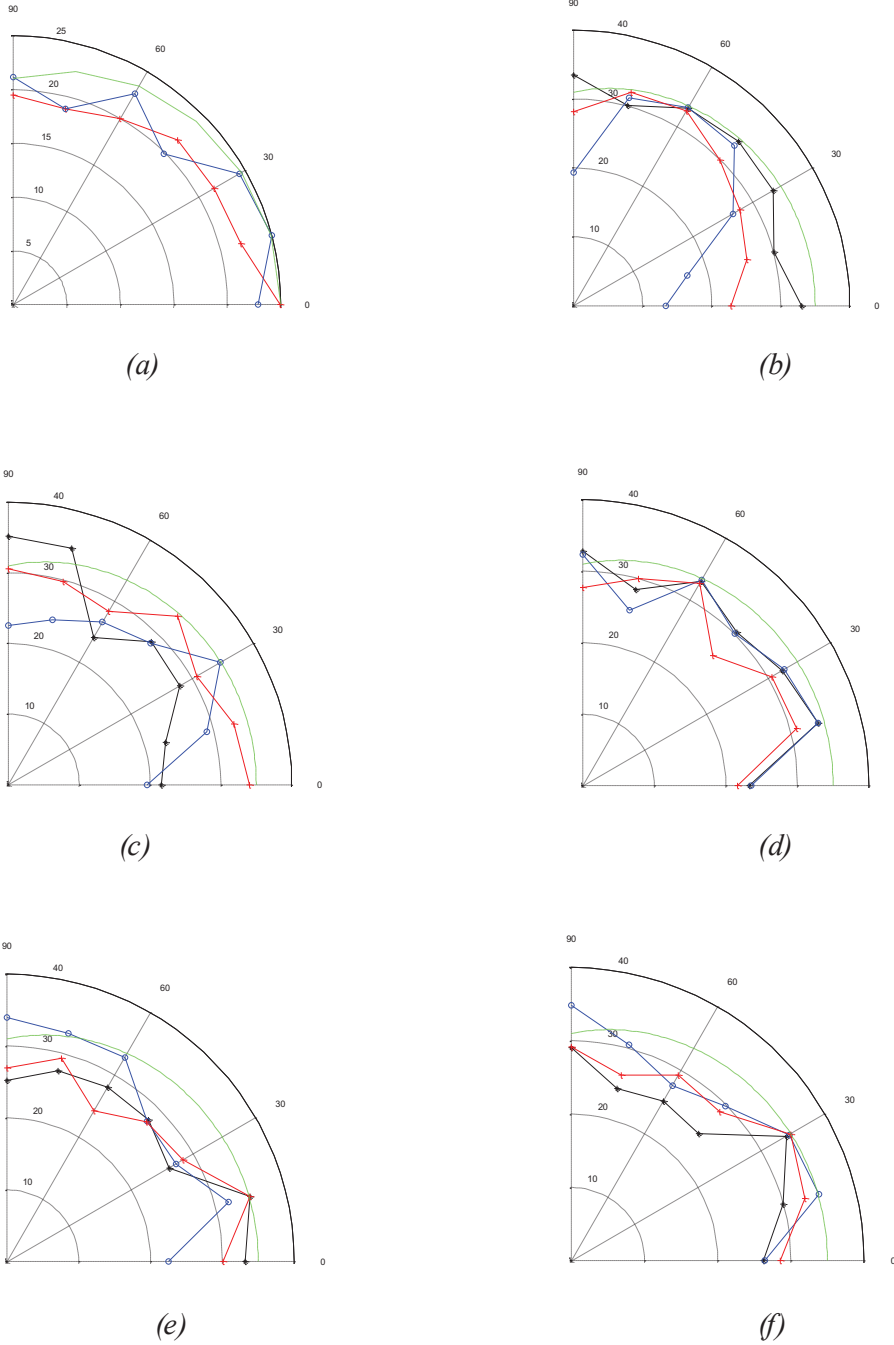


FIGURE 6-13 Directivity of an NS Intercity wheel for one-nodal-circle axial modes. The wheel axis lies at the angle 0° , angles greater than 90° represent positions behind the wheel. —, $n = 3, 2740\text{ Hz}$; ---, $n = 5, 3850\text{ Hz}$, adapted from [6.14]

(c)

Fig. 2.12. The directivity of wheel radiation reported by Thompson, which was measured by TNO [4]. (a) Measurement setup. (b) The directivity of radial modes. (c) The directivity of axial modes. The wheel has a straight web.



*Fig. 2.13. The horizontal directivity of wheel noise (SJ 57H freight car wheelset, see Fig. 1).
(a) The directivity of A-weighted total level; —, excited laterally; —, excited vertically;
—, the simulation function $25+10 \lg[0.4+0.6 \cos(\psi)]$, (b)~(f) the directivities in one-third octave bands, excited vertically: (b) —, 315 Hz; —, 400 Hz; —, 500 Hz; —, the simulation, (c) —, 630 Hz; —, 800 Hz; —, 1000 Hz; —, the simulation, (d) —, 1250 Hz; —, 1600 Hz; —, 2000 Hz; —, the simulation, (e) —, 2500 Hz; —, 3150 Hz; —, 4000 Hz; —, the simulation, (f) —, 5000 Hz; —, 6300 Hz; —, 8000 Hz; —, the simulation. (The simulation function is $35+10 \lg[0.4+0.6 \cos(\psi)]$.)*

As has been analysed in [48], for railway wheels with a curved web, radial modes and axial modes are well coupled. Since this coupling must be much less effective for wheels with a straight web, radiation directivity of this wheel type may differ from that of wheels with a curved web.

2.4 Some discussion

The directivity of wheel radiation is likely close to that of a monopole source for wheels with a curved web, based on the directivity data reported by Remington, measured by SP (Fig. 2.13(a)) and discussed in [48]. For wheels with a straight web, radiation directivity of axial modes could be close to that of a dipole source, based on the narrow band wheel directivity reported in [48]. However, the directivity data contain strong interference effects, as shown in Fig. 2.12(b) and 2.12(c). Thus, re-inspection of the directivity could be necessary.

Interference between direct sound and ground reflected sound can be alleviated by covering the ground in absorptive material. However, interference also exists between direct sound rays emitted from different parts of a vibrating wheel. By using a larger measurement radius interferences between different direct rays could be alleviated as Remington's directivity data could suggest. A larger measurement radius can also reduce the effect of source dimension on the directivity because the open angle of a wheel to a receiver further away becomes smaller. Thus, a measurement radius about 4~6 times the wheel diameter is proposed in Paper III, of which the upper limit is based on the consideration of having a good signal-to-noise ratio. Radiation directivity of wheels with a straight web shall then be re-inspected both in narrow bands and in one-third octave bands using such a measurement radius. The reason to measure it in one-third octave bands is simply due to the fact that railway noise engineering requires directivity data of this type.

2.5 Measurement of locomotive noise

2.5.1 Locomotive noise when stationary

In 2001, SP Acoustics measured the (stationary) sound power level of a diesel-electric locomotive in Oxelösund, Sweden. The locomotive is EMD type JT42CWR, Class 66 in GB, modified to comply with Swedish requirements, as shown in Fig. 2.14. The relevant technical data are given below:

| | |
|-----------------|---|
| Diesel motor | GM 12N-710G3B-EC |
| Main generator | GM AR8/CA6 |
| Traction motors | GM D43 TR |
| Effect motor | 3200 BHP (Brake horse power) |
| Effect traction | 3000 THP (Traction horse power, ~ 2200 kW; ~ 900 rpm) |
| Axle series | Co Co |
| Length | 21.5 m |
| Width | 2.65 m |
| Height | 3.93 m |



Fig. 2.14. The measured diesel-electric locomotive of GB T66 type. In the picture the long-side 2 is shown, which was facing the sea when its sound power was measured.

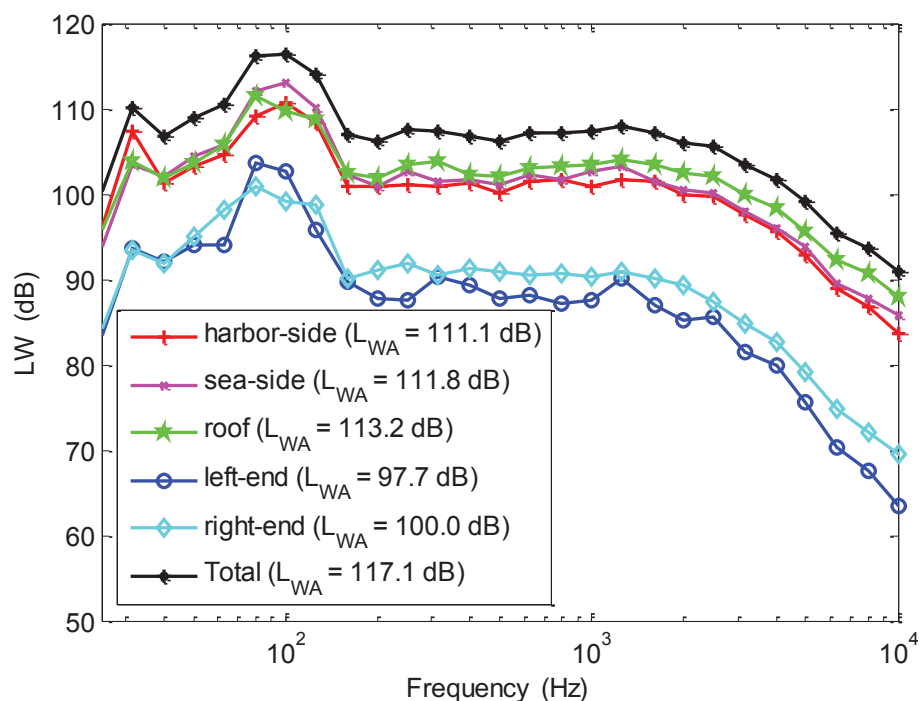


Fig. 2.15. The sound power levels of the diesel-electric locomotive, measured at stationary and at full power (900 rpm / 2208 KW). (The right side means the right side when facing the sea.)

Using a box-shaped measurement surface according to ISO 3746, the sound power level is measured when the locomotive is stationary on a concrete ground in the harbour and the engine runs at its full power (900 rpm). Based on the measured data shown in Fig. 2.16, the sound power levels on each side surface and on the top surface of the measurement box are each determined as shown in Fig. 2.15. The total sound power level is of a nearly constant level from 31.5 to 2000 Hz (like pink noise), except the distinctive peak around 100 Hz that is about 9 dB higher. Above 2000 Hz the sound power level drops quickly with frequency, which is likely due to the acoustical measure of sound absorption applied in the engine chamber and at the ventilation channels. By the way, this level of the total sound power shows that this type of diesel-electric locomotives is one of the quietest.

| Harbour-side-middle (3 m) | Harbour-side-top (6 m) | Left-end middle (3 m) 77.9 | Sea-side-top (6 m) | Sea-side-middle (3 m) |
|---------------------------|------------------------|--------------------------------|--------------------|-----------------------|
| | 82.2 | | 83.3 | |
| 86.2 | | 83.9 | | 86.2 |
| | 87.8 | | 88.8 | |
| 89.6 | | 91.6 | | 91.0 |
| | 92.8 | Roof + 2 m | 92.7 | |
| 90.8 | | 97.3 | | 92.7 |
| | 92.6 | | 92.0 | |
| 86.6 | | 90.6 | | 88.7 |
| | 84.4 | | 86.1 | |
| | | 78.7 Right-end middle (3 m) | | |

Fig. 2.16. A-weighted sound power levels of GB T66 locomotive noise, in dB(A), measured by SP Acoustics. The sound power levels are measured on a box-shaped surface which is about 2m to the locomotive surface.

2.5.2 Locomotive noise vs. rolling noise

To compare the traction noise of this locomotive with the rolling noise, a few specially designed pass-by measurements have been carried out on a track at Nykyrka in Nyköping which has a speed limit of 80 km/h and is not used for public traffic: two pass-bys of constant speeds of 45 or 79 km/h and two other pass-bys under full acceleration to speeds 39 or 70 km/h when the locomotive reaches the position in front of the measurement microphone which is located 25 m from the nearest rail. The locomotive is 21 m long and carries a 1,018 tonne load (9 cars loaded with iron blocks and 5 cars loaded with containers). The total train length is 215 m.

The pass-by results are shown in Fig. 2.17. As can be seen, (1) the locomotive noise at full traction power dominates around 100 Hz because of the 9 dB high peak in its power; (2) the locomotive noise at full traction power also dominates $L\text{-max}$ values at 250 and 1250 Hz during the pass-by under full acceleration to 39 km/h, compared with $L\text{-max}$ levels of the pass-by at constant speed 45 km/h; (3) above 200 Hz rolling noise becomes dominant for speeds above about 50 km/h. The sound pressure level at the microphone produced by the locomotive noise is calculated using the formula for a point source:

$$L_{p,loco} = L_{W,loco} - 10 * \log_{10}(4\pi * 25^2) + L_{excess} \text{ (dB)}, \quad (2-1)$$

where the excess attenuation, L_{excess} , is approximately 5 dB at low frequencies for most of terrains (evaluated using the Nord 2000 propagation model).

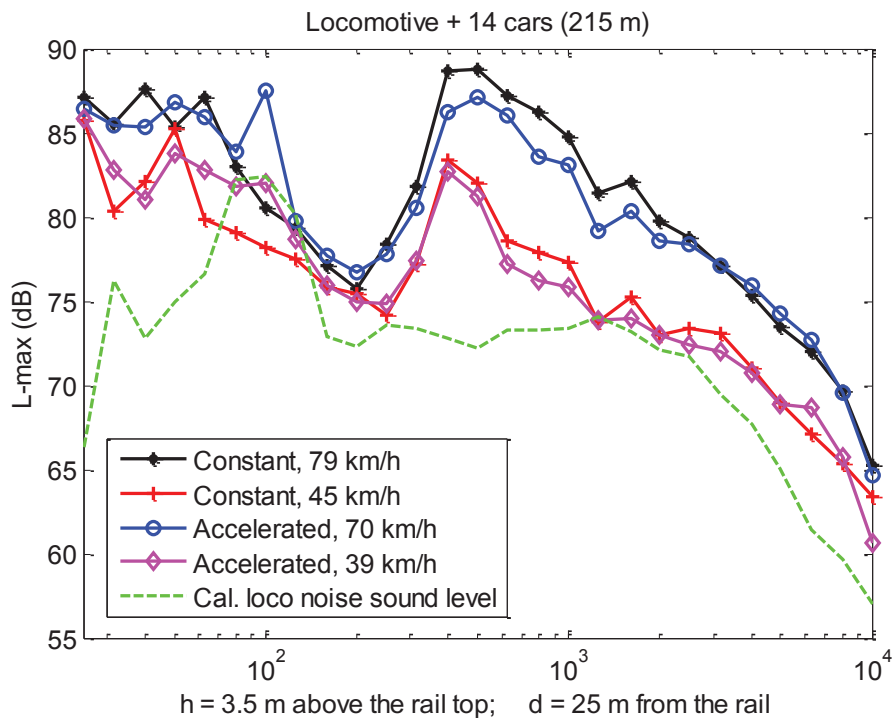


Fig. 2.17. The effect of locomotive noise on the pass-by noise ($L\text{-max}$)

2.5.3. *The directivity*

According to the measured sound power levels shown in Fig. 2.15, the sound power emitted into the forward or backward direction is more than 10 dB lower than those emitted sideward or upward. As can be understood, the shielding effect by the two end walls is strong due to the fact that the two respective microphones are located at the middle of the end walls, 1 m under the roof and 2 m to the locomotive end surfaces. However, the shielding effect of the end walls will become less for receivers located further to the end walls. Moreover, considering the 9 dB peak level around 100 Hz, the directivity of locomotive noise at distant is as estimated negligible.

3 Directivity Description of Railway Noise

3.1 Rolling noise

Railway rolling noise has well been understood. Based on the model which is setup by Remington [5] and further developed by Thompson [4], the noise generation mechanism can schematically be described by a block diagram below:

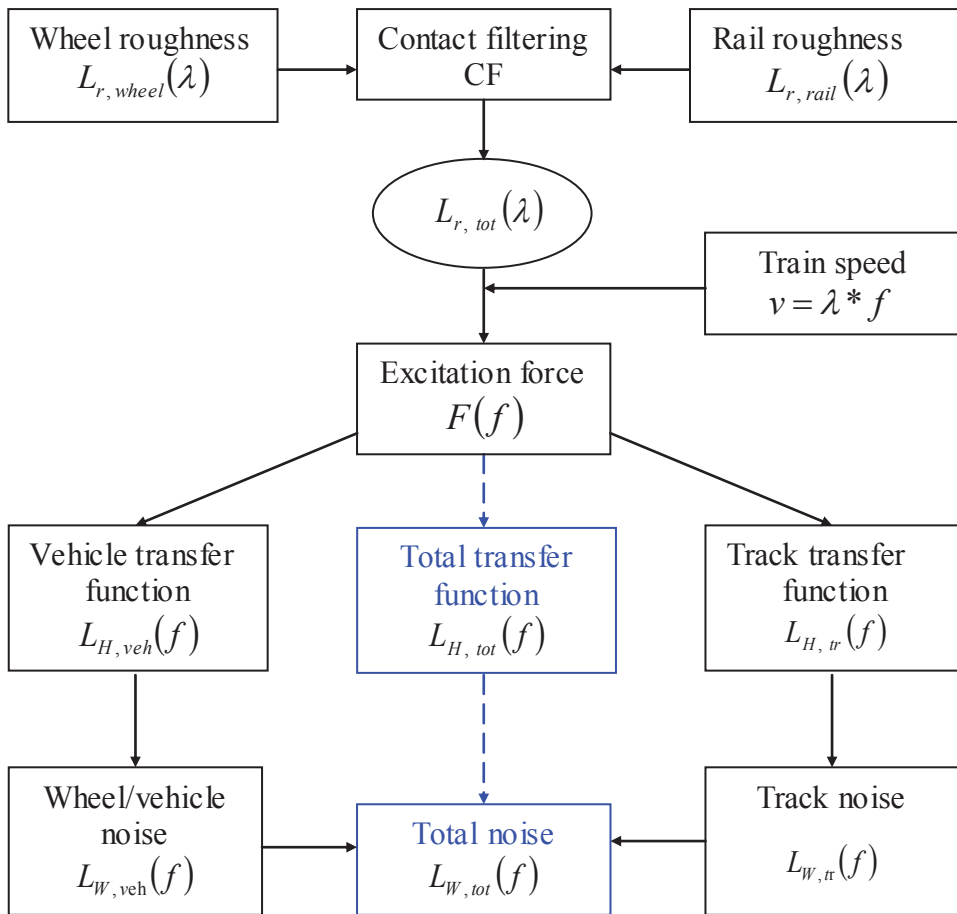


Fig. 3.1. Block diagram of the modelling process of railway rolling noise.

The model presented in Fig. 3.1 is in principle a linear model. However, by replacing the total roughness, $L_{r,tot}(\lambda)$, with an equivalent roughness [54-55], this model can be extended to handle impact sound where interaction between wheel and rail is non-

linear. (Note: with a suitable model, a non-linear excitation concerned with impact sound is to be transferred to respective equivalent roughness excitation.)

Within this noise generation mechanism, a transfer function inclusively describes the sound radiation efficiency and directivity. However, a proper directivity description of a sound source is handled outside of the procedure shown in Fig. 3.1, and is mainly based on measurement investigation (see the discussion in Paper V). In fact, in Remington's model the directivity of wheel and rail radiation is neglected; while, in Thompson's model, rail radiation in the horizontal direction is calculated by modelling the vibrating rail as a line of coherent monopoles.

As has been mentioned in section 1.2, the understanding of the directivity of rolling noise is not unified although it has been studied for about 40 years. The difficulty is mainly two aspects. On the one hand, the horizontal directivity of rail radiation cannot be measured directly because of the physical feature that a vibrating rail is only slightly decayed (in the important frequency range). On the other hand, when measuring the directivity of wheel radiation, strong interferences seriously distort the directivity pattern. As a consequence, it seems that there are controversies in handling the noise sources. Should pass-by rolling noise be modelled as a line of *coherent* monopole sources, or a line of *incoherent* dipole sources? Is a vibrating railway wheel a dipole source, or a source close to a monopole? Some numerical model analyses tried to address these problems [48-49]; while, it seems that, in itself, the numerical models are unable to give convincing answers.

One other issue is vertical directivity of train pass-by noise, which is especially important when predicting noise impact from rail vehicles on near line high-rise buildings. However, this quantity varies when people measure it at different sites [44-46], because it can be affected by many factors such as the shielding of the car body, ground reflection and absorption, the shielding and/or reflection and/or diffraction of nearby constructions, and the radiation of the vibrating foundations such as a vibrating viaduct or bridge.

Considering that, during a train pass-by, excitations at different wheel-rail contact points are incoherent, it then seems proper to model pass-by rolling noise as a line of incoherent point sources of certain directivity characters. This directivity in the horizontal direction and at conventional speed can, based on Peters' investigation where pass-by noise of a train at 144 km/h was studied [39], be simulated as [41],

$$10 \lg[0.15 + 0.85 * \cos^2(\varphi)], \quad (3-1)$$

where angle φ is defined as shown in Fig. 1.1. This directivity is close to that of a dipole source.

Train pass-by noise is a line source; the source length is nearly the same as the train length which varies from train to train. A passenger train can have a length from about 50 m to more than 300 m. And, a freight train is usually much longer than a passenger train. Extremely long freight trains can have a length longer than 3,000 m. Therefore, as for railway noise engineering (noise measurement or noise prediction), a receiver's distance to the track concerned is often less than the train length. In other words, horizontal directivity of pass-by rolling noise varies with the receiver's position. This

problem has been investigated in Paper I. The discussion of this issue is re-formulated and presented in Annex A, with some practical examples provided.

The directivity of wheel radiation is analysed based on SP's measurement investigation of the problem [40], and by referring to the relevant discussions made by others [5, 39, 48]. Discussions made in [48] in particular indicate that directivity of wheel radiation could be different for wheels with a curved web compared with those with a straight web. Railway wheels with a curved web are popular in use; and, available measurement studies on the radiation directivity of this wheel type are consistent [5, 41, 48]. Thus, for wheels with a curved web, a more or less frequency independent directivity is proposed as [41, 43, or Papers II, III and V]

$$\Delta L_{\text{wheel}}(\varphi) = 10 \lg[0.4 + 0.6 * \cos(\varphi)]. \quad (3-2)$$

For those wheels with a straight web, directivity of wheel radiation could be close to that of a dipole source. While, as the directivity data of this wheel type reported in [48] contain a strong effect of interference, further investigation using a larger measurement radius is proposed in Paper V. Moreover, it is also proposed that, not only at the wheel's natural frequencies, but also in one-third octave bands, directivity shall be investigated as well because railway noise engineering requires data of this type.

All measurement investigations on vertical directivity of rail radiation [5, 41, 47] reach the similar conclusion: it is close to that of a monopole source. Based on SP's directivity data this vertical directivity is simulated by [41, 43, or Papers II, III and V]

$$\Delta L_{\text{v}}^r(\psi) = 10 \lg[0.4 + 0.6 * \cos^2(\psi)], \quad (3-3)$$

where ΔL_{v}^r denotes the vertical directivity of rail radiation and ψ is the vertical angle for pass-by noise as shown in Fig. 1-1. As can be seen, this directivity function differs slightly from that given by Eq. (3-2).

Horizontal directivity of rail radiation cannot be measured directly because of the physical feature that a vibrating rail is a line source. Based on Peters' estimation of the horizontal directivity of pass-by rolling noise [39], together with the directivity of wheel radiation specified by Eq. (3-2), it is assumed that rail radiation is of a dipole directivity character. Consequently, a calculation procedure to determine the horizontal directivity of rolling noise, ΔL_{H}^R , is proposed [43, or Papers III and V]

$$\Delta L_{\text{H}}^R(\varphi, f) = \begin{cases} D_{\text{wheel}} \oplus \{L_{\text{H,tr}}(f) - L_{\text{H,veh}}(f)\}, & f \leq f_{\text{de}} \\ D_{\text{wheel}} \oplus \{D_{\text{dipole}} + L_{\text{H,tr}}(f) - L_{\text{H,veh}}(f)\}, & f > f_{\text{de}} \end{cases} \quad (3-4)$$

where D_{wheel} is given by Eq. (3-2), $D_{\text{dipole}} = 10 \lg[0.001 + 0.999 * \cos^2(\varphi)]$ is a practical form of dipole directivity function, f_{de} the de-coupling frequency of the

track, $L_{H, \text{veh}}(f)$ the vehicle transfer function, $L_{H, \text{tr}}(f)$ the track transfer function,
 \oplus denotes energy summation.

Relative strength in sound power between rail and wheel radiation shifts with speed. In general, rail radiation contributes more at low speed while wheel radiation becomes more important at high speed [4]. For example, according to a TWINS calculation, rail radiation is about 4 dB stronger than that of the wheels at 100 km/h (for the given train-track combination) [4]. A shift in relative strength between the two noise components directly changes the horizontal directivity of rolling noise. A calculation example is given in Paper V, where wheel radiation at 350 km/h is estimated to be about 1 dB stronger than rail radiation. Horizontal directivity of total rolling noise at this speed will then be

$$10 \lg[0.23 + 0.35 * \cos(\varphi) + 0.42 * \cos^2(\varphi)] . \quad (3-5)$$

Compared with Eq. (3-1), this directivity is about 2 dB less directional.

For a fast moving sound source the Doppler factor has to be considered. This factor is described as [56]

$$[1 - M * \cos(\theta)]^{-2(n+1)} = [1 - M * \sin(\varphi)]^{-2(n+1)} , \quad (3-6)$$

where $M = u/c$ is the Mach number, angle $\theta = \pi/2 - \varphi$ is relative to the track while φ relative to the lateral direction of the track. $n = 0$ is for a moving point monopole source, $n = 1$ for a moving volume monopole or force dipole source, $n = 2$ for a moving quadrupole source, and so on.

Thus, at high speed, effective horizontal directivity of rolling noise consists of two components

$$\Delta L_{H, \text{combined}}^R(\varphi, f) = \Delta L_H^R(\varphi, f) - 20 \lg[1 - M * \sin(\varphi)] , \quad (3-7)$$

where $\Delta L_H^R(\varphi, f)$ is determined by Eq. (3-4). In Paper V the first term in Eq. (3-7), $\Delta L_H^R(\varphi, f)$, is named as *source term* because it depends on the directivity character of a sound source. And, the Doppler factor is named as *motion term*. An example of such effective horizontal directivity is given in Fig. 3.2.

Vertical directivity of pass-by rolling noise is in fact still a problem. Eq. (3-2) or Eq. (3-3) only describes the vertical directivity of wheel-rail vibration noise. As has been mentioned before, the vertical directivity of rolling noise can be affected by many factors: the shielding of the car body, ground reflection and absorption, the shielding and/or reflection and/or diffraction of nearby constructions, and the radiation of the vibrating foundations such as a vibrating viaduct or bridge. Therefore, it seems impossible to work out a general directivity function for engineering applications. What can be considered at this time are empirical directivity functions for categorized situations, which could be worked out based on extensive measurement investigation.

To understand the measurement specified directivity characteristics of wheel and rail radiation, a model of *perpendicular dipole pair* (PDP) is proposed, as presented in Papers IV and V. The modelling is started with a close inspection of the directivity pattern of a dipole source ($\cos^2(\phi)$). As is shown in Fig. 3.3, a free dipole presents dipole directivity character in a plane containing the dipole axis. However, in a plane perpendicular to the dipole axis, the free dipole presents a monopole directivity character! This fact suggests that, when considering the directivity effect of a dipole source, the orientation of its axis needs to be specified. Thus, as shown in Fig. 3.4, in modelling the directivity of rail radiation, a straight line of dipoles with vertical orientation (the blue arrows) simulates rail head and foot vibration, while a straight line of dipoles with lateral orientation (the red arrows) simulates rail web vibration. And, the latter is assumed to be about 4 dB stronger in sound power than the former.

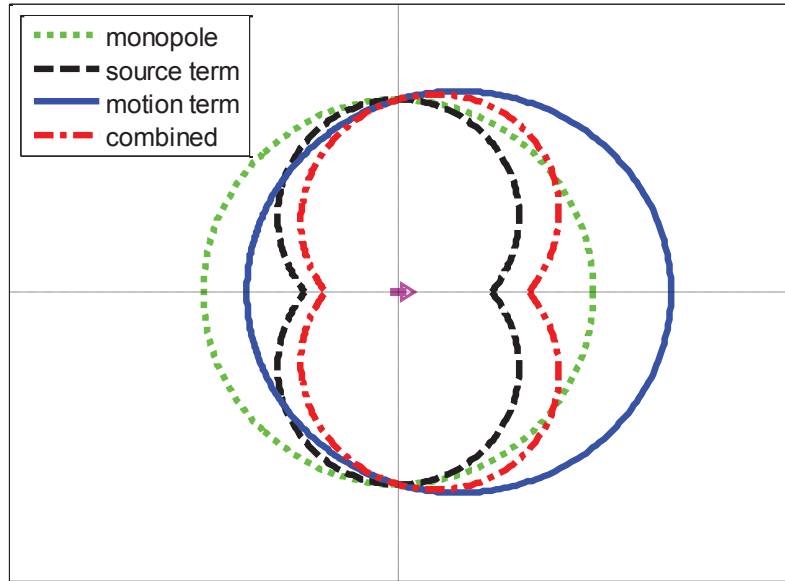


Fig. 3.2. The horizontal directivity of rolling noise at 350 km/h. The “source term” is given by Eq. (3-5) wherein wheel radiation has been assumed 1 dB stronger than rail radiation. The “combined” is given by Eq. (3-7) and “motion term” is the second term on the right hand side of Eq. (3-7).

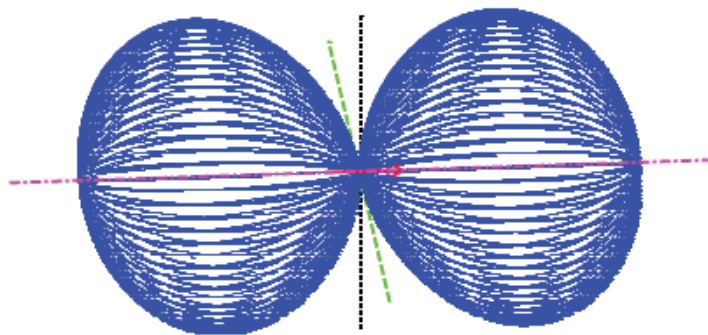


Fig. 3.3. 3D directivity character of a free dipole

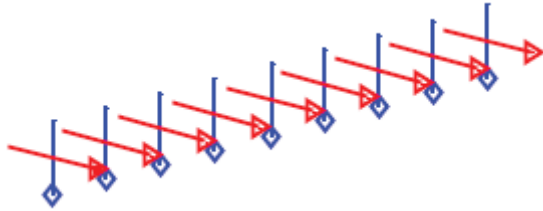


Fig. 3.4. A straight line of perpendicular dipole pairs used to model directivity of rail radiation

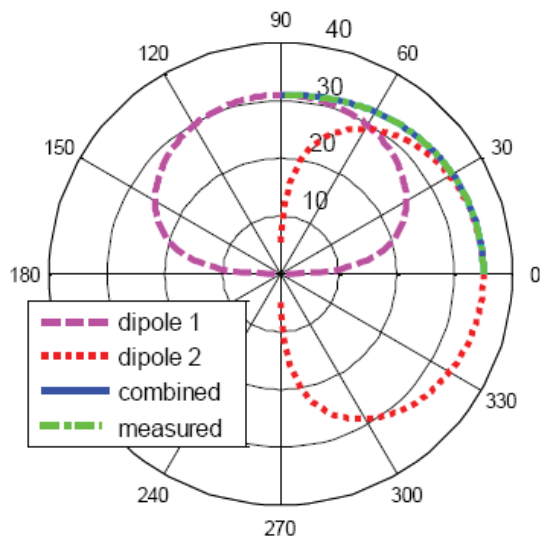


Fig. 3.5. Comparison between measured vertical directivity of rail radiation and the one predicted by the model of perpendicular dipole pair, “combined”, where the directivities of dipole 1, dipole 2, and “combined” are given by Eqs. (7) to (9) in paper V, respectively.

In a horizontal plane located at about half the rail height, the line of dipoles with vertical orientation presents a monopole directivity character (and is of negligible sound power), while the line of dipoles with lateral orientation presents a dipole directivity character. The combined horizontal directivity of the dipole pair is of dipole character. However, in a vertical plane perpendicular to the rail, they both present a dipole directivity character. Thus, the combined vertical directivity of the dipole pair depends on the relative strength in their sound powers. Based on the calculation shown in Paper V, the numerical result shown in Fig. 3.5 indicates that the PDP model for rail radiation produces a vertical directivity identical to the one given by Eq. (3-3). Thus, it has proved that the model of a straight line of PDPs can properly simulate both the vertical and horizontal directivity characteristics of rail radiation.

Modelling the directivity of wheel radiation is equivalent to modelling that of rail radiation because of the relation between their geometries: to bend a rail section to a circle will geometrically form a wheel. Thus, a straight line of PDPs for modelling rail radiation becomes a circular line of PDPs for modelling wheel radiation, as shown in Fig. 3.6. Due to the symmetry in wheel’s geometry, emitted sound power of a vibrating wheel is circularly the same while it can be different in a plane containing

the wheel axle; this plane is the correspondent of a vertical plane perpendicular to the rail in which the radiation directivity is close to that of a monopole. Therefore, this model naturally explains why a vibrating railway wheel is not a dipole source.

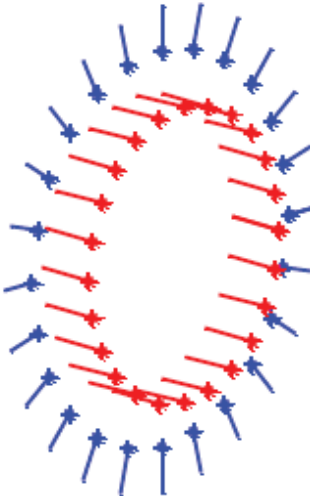


Fig. 3.6. A circular line of perpendicular dipole pairs used to model directivity of wheel radiation

In addition, a finite line of dipoles will present a dipole directivity character in the horizontal direction for a distant receiver. For a receiver which is close to the finite line source and located near the middle of the source line, radiation of the line source points to the normal direction of the source line. Moreover, in the modelling, a closed circle equivalently corresponds to an infinite long line source (which is free from the effect of ends); therefore, wheel radiation has a circular uniform distribution.

3.2 Aerodynamic noise

Measurement study of railway aerodynamic noise has made great advancements: all important noise components together with respective speed indices and relative strength between components' sound powers have been identified [29-31]. However, as for model calculation, there are only simple case studies simulating pantograph noise or fluid-cavity-interaction noise [34-37]. For dominant noise component around bogies where scattered fluid sound is the concern, there is no proper calculation method presently available [33]; therefore, only qualitative studies can be made. In general, for a problem of fluid-structure interaction, this is usually handled by computational fluid dynamics (CFD). As is briefly summarized in Annex B, complex flow simulations are challenging and error-prone; it takes a lot of engineering expertise to obtain validated solutions.

Fortunately, it has been found that a reliable quantitative description of railway aerodynamic noise is not necessary a condition for studying the directivity of relevant sources. In Paper V a systematic investigation into directivity characteristics of this noise type is presented. The study analysed a set of directivity data of pantograph noise, inspected the Harmonoise proposal for the directivity of the other sub-sources, referred to the theoretical solutions of two types of scattered fluid sounds and

proposed a different mechanism for aerodynamic sound generated around bogie areas. A distinct directivity description for this noise type was proposed as the output of the investigation.

A set of tabular directivity data of pantograph noise (for TGV-R trains) was reported in [30] although not analysed. Thus, this set of directivity data are analysed in Paper V. It has been found that the horizontal directivity of the pantograph noise can be simulated by

$$\Delta L_{\text{pantograph}} = 10 * \lg[0.006 + (1 - 0.006) * \cos^2(\varphi)], \quad (3-8)$$

$$\Delta L_{\text{Doppler}} = -40 * \lg[1 - M * \sin(\varphi)], \quad M = u / c, \quad (3-9)$$

$$\Delta L_{\text{combined}} = \Delta L_{\text{pantograph}} + \Delta L_{\text{Doppler}} \quad (3-10)$$

As is shown in Fig. 3.7(a), these equations can approximately re-produce the measurement specified horizontal directivity. Moreover, the source term given by Eq. (3-8) indicates that the pantograph noise is of a dipole directivity character in the horizontal direction.

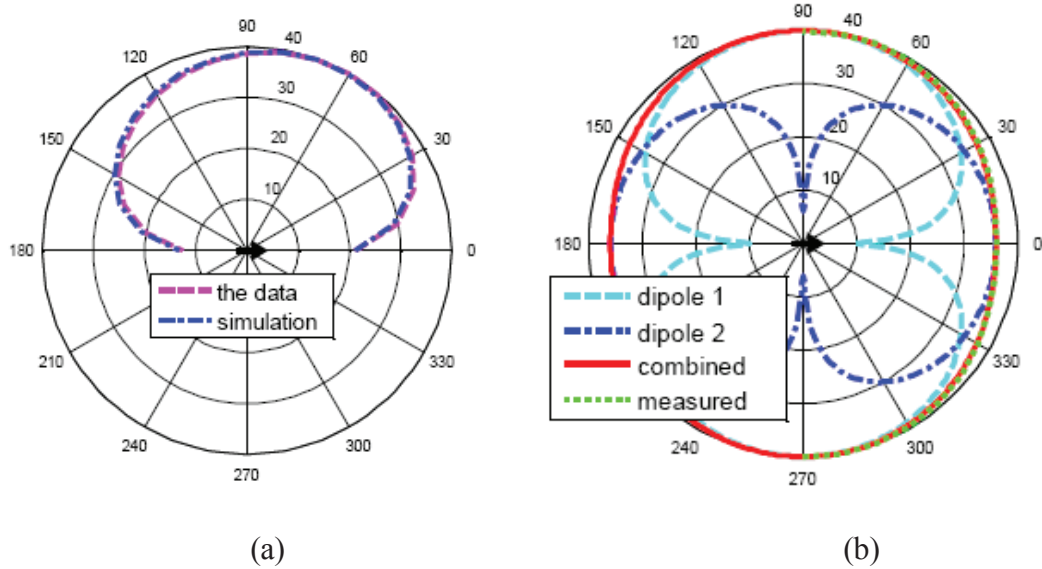


Fig. 3.7. (a) The measured horizontal directivity of pantograph noise [17] compared with the simulation directivity function formulated by Eqs. (3-8) to (3-10). (b) The measured vertical directivity of pantograph noise compared with the simulation of perpendicular dipole pair of which the dipole with lateral orientation is 4 dB weaker.

It is now necessary to discuss the physics behind the phenomenon. Pantograph noise is caused by the vortex-induced vibration (VIV) which under certain conditions can cause Aeolian sound if the frequency of vortex shedding matches the resonance frequency of the structure [57]. Aeolian sound is a dipole source [56], with an orientation transverse to the flow and the sliding bow; hence, the VIV sound is a

dipole source of vertical orientation. Thus, the VIV sound should present a monopole directivity character in the horizontal direction. Therefore, to be of the horizontal directivity given by Eq. (3-8) requires a dipole source with lateral orientation. In other words, this second dipole source is perpendicular to the dipole source of the first VIV sound. It is not clear to me what mechanism generates this second dipole source. It could be the interaction between the air flow and the two end parts of the sliding bow that induces a lateral vibration, compared with the lift force on the middle part of the sliding bow where the first VIV sound is induced. Or, probably, the total VIV sound in this case contains comparable vertical and lateral components due to the shape of the sliding bow of a pantograph.

Once again, we find the third example of a perpendicular dipole pair. In fact, PDP is a useful concept. For example, with the understanding that pantograph noise is of PDP components, i.e. the vertical and lateral components of the VIV sound, the measurement specified vertical directivity of the pantograph noise becomes easy to explain. By assuming that the vertical component of the VIV sound is about 4 dB stronger than the lateral component, the vertical directivity can be re-produced as shown in Fig. 3.7(b).

Measurement investigation [30] confirms that turbulent boundary layer noise is less important compared with other aerodynamic noise components. However, it is worth discussing this noise type a little more in detail because it is an aerodynamic noise component which has been solved analytically by Tam [58].

As has been shown in Paper V, the directivity of turbulent boundary layer noise in a plane perpendicular to the flow can be simulated by

$$\Delta L^P(\varphi) = 10 \lg[0.001 + 0.75 * \cos(\varphi) + (0.25 - 0.001) * \cos^2(\varphi)]. \quad (3-11)$$

This directivity function describes a sound source which is slightly less directional than a dipole.

When comparing Eq. (3-11) with the Harmonoise proposal for the directivity of aerodynamic sources other than pantograph noise,

$$5 * \ln[\sin(\varphi + \pi/2)], \quad (1-1)$$

it has been found that these two directivity functions are numerically the same, see Fig. 3.8(a). Thus, the Harmonoise proposal for the directivity of aerodynamic noise is in fact for that of turbulent boundary layer noise. In the following, it will be shown that this proposal seems to be incorrect because the dominant component of aerodynamic noise, scattered fluid sound around bogies, is of a directivity character different from that given by Eq. (1-1).

Aerodynamic sound generated around bogie regions has been identified to be the most important component of railway aerodynamic noise; its generation mechanism is assumed to be flow separation and recirculation [29-30]. However, it seems that *scattering* of the air flow is the dominant mechanism for the phenomenon. As for

scattered fluid sound, the theoretical solution shows that it is a dipole source with the dipole axis in the downstream direction [56].

Turbulent boundary layer noise along the side walls of a train and scattered fluid sound around the bogies are the perpendicular components of the fluid-structure interaction noise. Since turbulent boundary layer noise is approximately a dipole source, thus, they are again a PDP source and can be treated in a similar way.

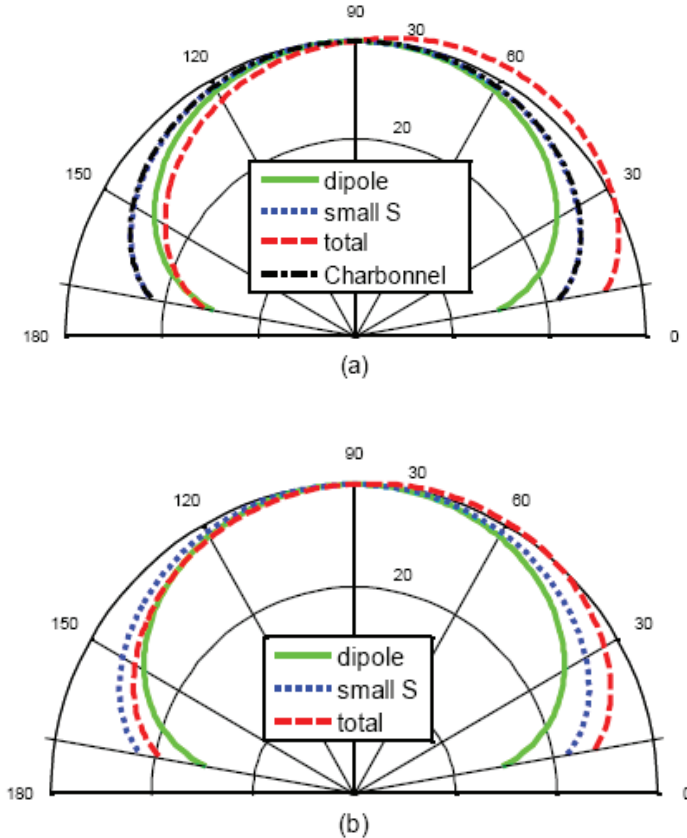


Fig. 3.8. Comparison between various directivity functions: “small S” denotes the directivity for small Strouhal number components given by Eq. (19) in paper V; “total” is the tilted total directivity of turbulent boundary layer noise simulated by Eqs. (19) to (21) in paper V. (a) $M = 0.7$; “Charbonnel” denotes the directivity proposed by Charbonnel, given by Eq. (15) in paper V, which overlaps the directivity of “small S”; (b) $M = 0.29$ ($V = 350$ km/h). 0° is for downstream direction.

The combined horizontal directivity of this PDP source could easily be constructed if the relative strength in sound power between the two dipole components were known. However, this information is presently not available. Thus, an estimation is made. If the scattered fluid sound is assumed to be 15 dB stronger in sound power than the turbulent boundary layer noise, the combined horizontal directivity will be

$$\Delta L_H^A(\varphi) = 10 * \lg[C_1 + (1 - C_1) * \cos^2(\varphi - \pi/2)], \quad C_1 = 0.03, \quad (3-12)$$

where the horizontal angle, φ , is relative to the lateral normal, as shown in Fig. 1.1. This directivity function indicates that, for the combined horizontal directivity of the

perpendicular dipole pair, turbulent boundary layer noise is equivalent to a small monopole component described by C_1 . Moreover, if the difference in sound power between the two dipole components is 10 or 20 dB, there will be $C_1 = 0.1$ or $C_1 = 0.01$, respectively.

Since aerodynamic noise will be only important at high speed, the Doppler factor, i.e. the motion term, needs to be considered. The effective combined horizontal directivity of aerodynamic noise (not including pantograph noise) is then given by

$$\Delta L_{H,\text{combined}}^A(\varphi) = \Delta L_H^A(\varphi) - 40 * \lg[1 - M * \sin(\varphi)], \quad (3-13)$$

where the source term, $\Delta L_H^A(\varphi)$, is given by Eq. (3-12) if turbulent boundary layer noise is 15 dB weaker. This effective combined horizontal directivity at 350 km/h is depicted in Fig. 3.9. As can be seen, due to the effect of the Doppler factor, most sound power of the source is emitted in the forward direction.

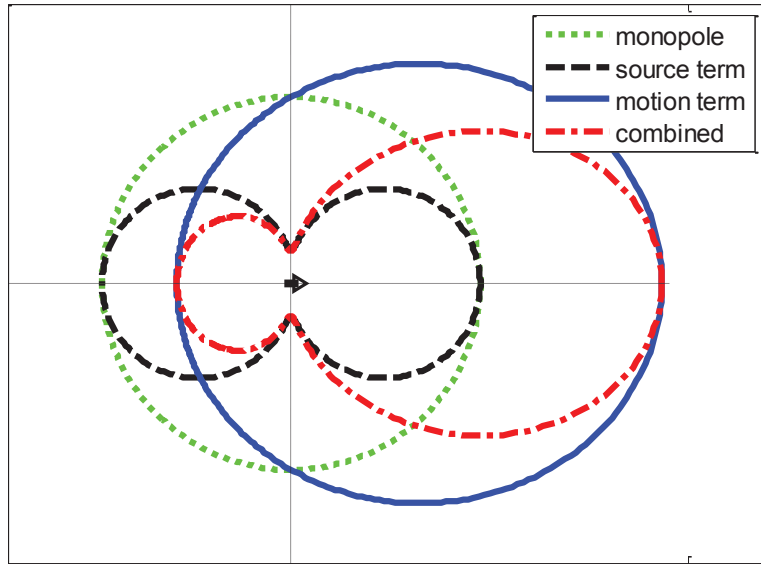
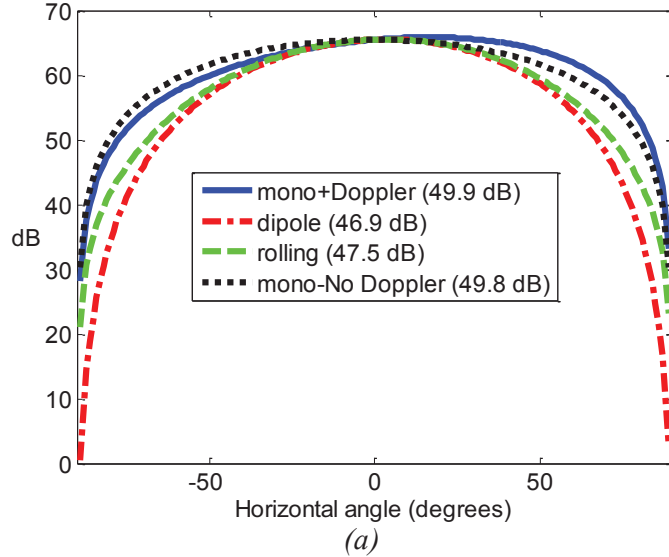


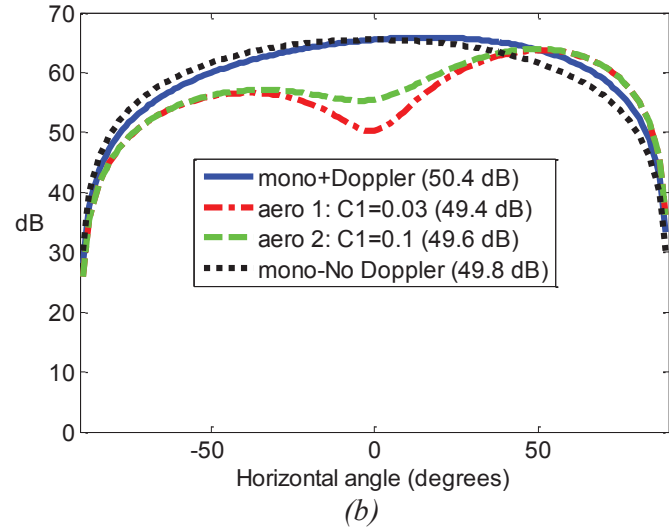
Fig. 9. The horizontal directivity of scattered fluid sound and boundary layer noise at 350 km/h. The “source term” is given by Eq. (3.12). The “combined” is given by Eq. (3.13) and “motion term” is the second term on the right hand side of Eq. (3.13).

The directivity character of scattered fluid sound suggests a possibility to separate aerodynamic noise around bogies from the rolling noise. If we consider a train speed of about 350 km/h at which aerodynamic noise and rolling noise are likely comparable [29]. Let us also assume that (for some wagons) pantograph noise is less important or can be separated. Thus, rolling noise dominates in the lateral normal direction while scattered fluid sound dominates in the direction of motion, due to their directivity characters. To record railway noise at or near these two special angle positions will probably achieve the separation of the two noise components.

Some authors claim that “the detailed directivity is of little practical relevance. It is sufficient to obtain an indication of the approximate nature of the directivity” [49]. According to the context in [49] “the approximate nature of the directivity” means the monopole or dipole directivity character. This statement can be accepted if only rolling noise is concerned. However, as can be seen in Fig. 3.10, a proper directivity description of aerodynamic noise (other than pantograph noise), the dipole pairs together with the relative strength in their sound powers, is obviously important when predicting pass-by noise levels of the noise type.



(a)



(b)

Fig. 3.10. Pass-by sound pressure levels of a point source of certain directivity pattern. A receiver is located 150 m from the track. $L_p(\varphi) = L_0 - 10\lg(4\pi r^2) + dL(\varphi)$, where $L_0 = 120$ dB is taken and $r = 150 / \cos(\varphi)$. For simplicity excess attenuation is neglected. In (a) $dL(\varphi)$ is given by Eq. (3-7) with $u = 150$ km/h and in (b) $dL(\varphi)$ is given by Eq. (3-13) with $u = 350$ km/h. “No Doppler” means that the Doppler effect is not included; “rolling” means that Eq. (3-1) is applied. Moreover, 90° is the direction of motion. Digits in brackets are the respective total levels of pass-by noise.

3.3 Other important noise types

Important sources of railway noise other than rolling noise and aerodynamic noise are traction noise, impact sound, curve squeal, brake noise and bridge vibration noise [4].

In the past, traction noise could be important even up to 200 km/h [38]; today it is a dominant noise type at low speed. For example, SP has measured the noise sound power of a diesel-electric locomotive of GB T66 type. It has been found that, when the locomotive runs at its full traction effort, the traction noise cannot beat the rolling noise at 40 km/h (Fig. 2.17). Obviously, modern traction units are much quieter than old ones. Moreover, for modern traction units, the dominant traction noise sources are cooling fans and traction engine/motor(s). This understanding has been confirmed by a recent investigation into noise emission [52].

As for engine noise, considerable variations in sound power between engines of the same combustion system are “still not fully understood in spite of the large amount of theoretical and analytical work that has been carried out” [38]. As for fan noise, the mounting connection or/and housing condition can have significant influence on noise generation [38, 59]. This wide variation in sound power impedes a universal description in modelling traction noise, as neither the sound power nor the directivity can be formulated in a general manner.

Based on measurement, the monopole directivity is estimated for diesel-electric locomotive noise due to the typical high peak around 80-125 Hz in its sound power [38, 51]. For cooling fan noise, the type of a fan and manner of mounting may affect the directivity pattern. Thus, the directivity of cooling fan noise shall be worked out by measuring and analysing the spatial distribution of its sound field. One such example is obtained: the directivity data reported by Czolbe and Hecht [52] in which cooling fan noise dominates can be approximated by

$$\Delta L_H^T(\varphi) = 10 \lg[0.25 + 0.75 * \cos(\varphi)]. \quad (3-14)$$

Since a wide spread in sound power can be expected for various traction units, directivity data for each type of traction unit may need to be collected and analysed. However, the directivity of traction noise in general is probably not important, especially when integrated pass-by noise is concerned. For example, the directivity given by Eq. (3-14) will have the effect of [-0.5 1.1 2.0] dB at respective angle positions of [30° 45° 60°].

The directivity of impact sound should be the same as that of rolling noise. Braking at speed will produce broadband noise [60]; thus, the directivity of it should be the same as that of wheel radiation. Braking at very low speed will frequently induce brake squeal noise. Brake squeal and curve squeal noise may be of the same directivity character as that of wheel radiation, while caution should be observed as the directivity of wheel radiation has been determined based on the data in one-third octave bands and for wheels with a curved web. It is not clear if this directivity is also valid for a vibrating wheel with a straight web excited at a narrow frequency. To answer this question further measurement investigation is required.

There are two main reasons for noise amplification by a bridge: (1) because of its large radiation surface a bridge acts as a *sounding board*; (2) the rail itself may vibrate considerably greater than for track at grade [4]. Since a sounding board is likely to be less directional than a vibrating rail, the directivity of bridge noise differs from, while is likely less directional than, that of rail radiation. Presently, no such directivity data have been reported.

4 Conclusions and Future Works

Conclusions

Based on extensive and systematic investigations this thesis project has identified a proper and applicable directivity description of railway noise sources. The study focuses on the two most important noise types, i.e. rolling noise and aerodynamic noise. Directivities of other important noise types are also studied and directivity characteristics of these noise types become understood although lack the relevant directivity data. With all the outputs integrated, a survey of the directivities of all important railway noise sources has been achieved.

The basic directivity characteristics of wheel and rail radiation have been specified based on measurement investigation; and, these characteristics can be interpreted by the model of *perpendicular dipole pair* (PDP). Moreover, it has been found that pantograph noise is also of PDP components. Further, by applying the PDP concept, the directivity of other aerodynamic noise components can be handled by assuming the relative strength between the sound powers.

The horizontal directivity of rolling noise concerns the relative strength between wheel and rail radiation, which is speed dependent and described by the vehicle and track transfer functions. A general calculation procedure has been worked out to handle this horizontal directivity in one-third octave bands, given by Eq. (3-4).

The vertical directivity of wheel/rail radiation is given by Eq. (3-2), or equivalently, by Eq. (3-3), because the difference between these two functions is not important. However, in practice, the vertical directivity of railway noise which includes all important noise components is still an unsolved problem even for cases where rolling noise predominates. There are many factors which can significantly affect the equivalent vertical directivity. These factors can be the shielding of the car body, the shielding and/or reflection and/or diffraction of near-track objects such as low barriers or viaduct banks, radiation from vibrating foundations such as a vibrating viaduct or bridge, ground reflection and absorption. Therefore, vertical directivity shall in general be determined for each train type and even at each location if the terrains concerned differ a lot; no universal description for vertical directivity can be expected. Nevertheless, this quantity has to be handled because it is an important parameter for evaluating the noise impact from rail vehicles on near-line high-rise buildings. The area that could be improved in future would be a description of the vertical directivity for categorised situations, based on extensive measurement investigations.

The directivity of wheel radiation for wheels with a straight web could differ from that for wheels with a curved web. It is then proposed to re-inspect the directivity for this wheel type using a measurement radius 4~6 times the wheel diameter, and recording both in the wheel's natural frequencies (to see if axial and radial motion are decoupled) and in one-third octave bands (to see if there are dominant axial or radial modes in one-third octave bands).

Pantograph noise is also of PDP components, while only about 4 dB stronger in the vertical direction than in the train's lateral direction. This is probably due to the fact that the VIV sound is of vertical and lateral dipole components.

For aerodynamic noise around bogies, *scattering* of the air flow is proposed to be the dominant mechanism of the noise generation. Scattered fluid sound is a dipole source with the downstream orientation. Including the Doppler factor, most sound power of this important aerodynamic sound is radiated into the forward direction.

The directivity characteristics of rolling noise and the aerodynamic noise excluding pantograph noise present a possibility to separate railway aerodynamic noise around bogie areas from the rolling noise. If pantograph noise can be either separated or measured separately, this possibility should be useful for investigating and defining the sound power of railway aerodynamic noise.

Discussions on the directivities of other noise types, except traction noise, are mainly in principle and qualitatively due to the reasons that these noise types are related to wheel/rail vibration noise and that no such directivity data are presently available. These discussions provide insights into the directivity characteristics of these noise types and serve as a complement part to complete the survey of the directivities of important railway noise sources. However, the discussions are not intended for replacing necessary further measurement investigation on the directivities.

Measurement investigations into directivities of wheel-rail radiation and pantograph noise are the necessary and important parts in constructing the directivity description. However, the model of perpendicular dipole pair and theoretical solutions of scattered fluid sound play a critical role to reach a proper understanding of the directivity of railway noise and to complete the directivity description. Moreover, it has been found that, in themselves, the numerical models shown in [48-49] do not seem to be powerful enough to solve a directivity problem of this type.

Proposed future works

1. To separate railway aerodynamic noise around bogie areas from the rolling noise by utilizing their directivity characteristics. Ultimate Sound Probe (USP) [61] is probably a proper sensor to use for the purpose.
2. To develop applicable formulae to handle vertical directivity of train pass-by noise, focusing on different classified situations of near-line high-rise buildings.

Annex A Calculation Procedure to Determine the Equivalent Horizontal Directivity of A Line Source

A1. Angle integration

A1.1. A point source

For a point source moving rectilinearly along y-axis, its sound power, distance to a specified receiver and relevant excess attenuation are denoted by L_W , r and A_{excess} , respectively. The equivalent sound pressure level at the receiver during a travelling time T is given by

$$L_{eq} = 10 \lg \left(\frac{1}{T} \int_0^T \frac{10^{(L_W - A_{excess})/10}}{4\pi r^2} dt \right) = 10 \lg \left(\frac{1}{T} \int_0^T 10^{[L_W - 10 \lg(4\pi r^2) - A_{excess}] / 10} dt \right), \quad (A-1)$$

where $\lg = \log_{10}$. Assuming that, during the time interval T , the point source moves at a constant speed u from y_1 to y_2 as shown in Fig. A1, the integration then becomes

$$L_{eq} = 10 \lg \left(\frac{1}{y_2 - y_1} \int_{y_1}^{y_2} \frac{10^{(L_W - A_{excess})/10}}{4\pi r^2} dy \right) \quad (A-2)$$

Applying the transformation coefficient, $d\varphi/dy = d/(d^2 + y^2) = d/r^2$, where $d > 0$ is the distance to the track, the angle integration formula of the problem is obtained

$$L_{eq} = 10 \lg \left(\frac{1}{y_2 - y_1} \int_{\varphi_1}^{\varphi_2} 10^{[L_W(\varphi) - 10 \lg(4\pi d) - A_{excess}(\varphi)] / 10} d\varphi \right) \quad (A-3)$$

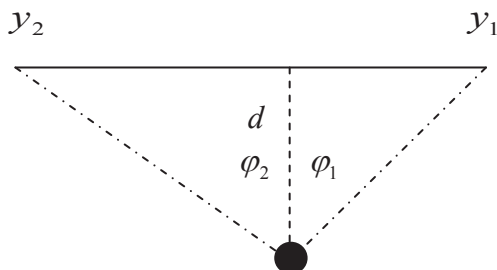


Fig. A1. Geometry for the calculation

A1.2. A line source

Assuming that the two ends of a stationary (or slowly moving) straight line source at time t are located at y_1 and y_2 , respectively. Instantaneous sound pressure level at the receiver is given by

$$L_p = 10 \lg \left(\int_{y_1}^{y_2} \frac{10^{(L_w - A_{excess})/10}}{4\pi r^2} dy \right) = 10 \lg \left(\int_{\varphi_1}^{\varphi_2} 10^{[L_w(\varphi) - 10 \lg 4\pi d - A_{excess}(\varphi)]/10} d\varphi \right), \quad (\text{A-4})$$

where it has implicitly assumed that the line source can be modelled as a line of incoherent point sources. Moreover, for simplicity, the effect of motion on horizontal directivity, the Doppler factor, is neglected in the calculation.

One advantage of angle integration is that, under free field condition ($A_{excess}(\varphi) = 0$), equal angular segments, $\Delta\varphi_i = \Delta\varphi$, will contribute the same to the sound pressure level L_p , provided that the line source consists of only monopole components ($L_w(\varphi) = L_w$). In the following discussions, in order to focus on the directivity of a sound source, free field condition of $A_{excess}(\varphi) = 0$ will be assumed. Thus, for a line source, if equal angular segments contribute differently to L_p , the line source must have a directivity character different from that of a monopole source.

A2. To define angle positions of a line source of finite length

For a point source, or when a measurement distance to the track is large compared with the source dimension, angle positions of the source can well be defined. However, when source dimension is considerable, a definition of angle positions of the source becomes flexible. For example, the geometrical centre of a source may be chosen to define angle positions of the source in relation to a receiver. Consequently, the directivity of a sound source can vary according to how the angle positions are defined; in other words, the way to define angles will have a *subjective* consequence although this consequence shall become negligible for a distant receiver. Railway rolling noise is such a line source, because a measurement distance to the track is often not large compared with the train length.

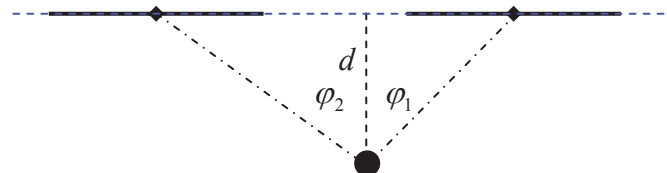


Fig. A2. The angle definition of a line source

For a line source of finite length, such as a passing-by train, its angle position in relation to a receiver can be defined with respect to some element of the source line, such as train front or middle, or other part like a pantograph, depending on if the chosen part to define angle positions of the source elements provides a convenient way of handling the problem. In this article, the *middle* of a line source will be taken as the reference element to define the horizontal angle, as shown in Fig. A2.

(Note: There will be no problem to define angle positions of each source element of a line source because they can well be modeled as point sources. However, it is often not practical in engineering to use multiple angle values to describe an angle position of a line source. And, unconsciously, people talk about horizontal directivity of train pass-by noise without mentioning the different receivers' distances to the track. All these are in fact concerned in the angle definition of a line source.)

A3. Angle positions of the source elements of a line source

As shown in Fig. A3, for a line source at a given angle position, say φ_j , (1) angle positions of its elements to a close receiver are different; (2) angle positions of a source element in relation to two receivers located at different distances are in general different. These differences in angles are the typical problem with such an angle definition when source dimension is considerable; and this is the reason why effective horizontal directivity of a line source varies with measurement distance. Only at distance (not less than the source dimension for a line source of uniformly distributed sound power) these differences in elements' angles become unimportant.

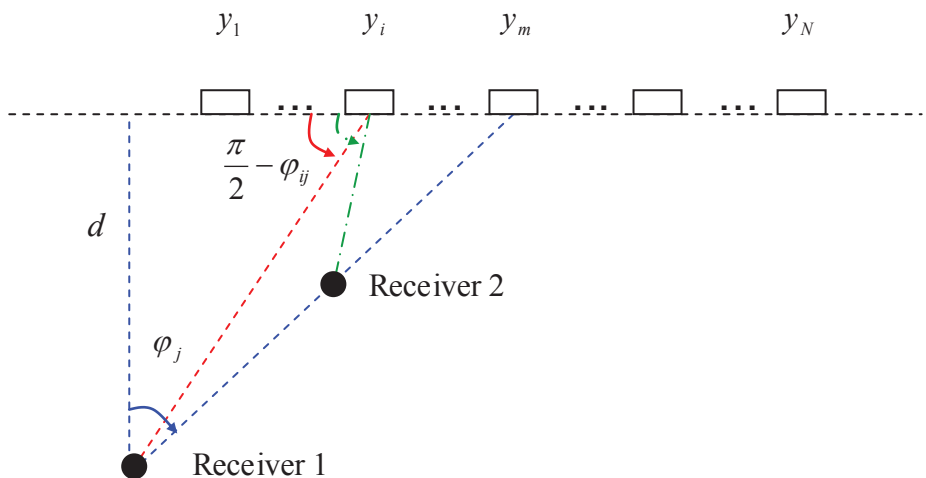


Fig. A3. Angle positions of a line source and its elements to receivers

In other words, the angle position of the reference source element in relation to the receiver is used to specify the angle position of the line source. However, if a receiver is not distant, respective angle positions of other source elements to the receiver will be considerably different from that of the reference source element. This problem of non-well-defined angles is typical in handling directivity of train pass-by noise.

A4. To express the directivity of a point sound source

In the horizontal direction, the sound power level of a point source can be written as

$$L_W = L_{W,0} + \Delta L_W, \quad (\text{A-5})$$

where $L_{W,0}$ is angle independent component in the sound power and $\Delta L_W = \Delta L_W(\varphi)$ is a function of horizontal angle, φ . When ΔL_W is normalized in the way

$$\frac{1}{\pi} \int_{-\pi/2}^{\pi/2} 10^{\Delta L_W/10} d\varphi = 1, \quad (\text{A-6})$$

then $L_{W,0}$ becomes the normalized sound power level. For a monopole source there is $\Delta L_W \equiv 0$. For a dipole source, if writing its normalized directivity as

$$\Delta L_{W,dipole} = C_0 + 10 * \lg(\cos^2 \varphi), \quad (\text{A-7})$$

It can be found that $C_0 = 10 * \lg(2) \approx 3$, or, the normalized directivity of a dipole source is $10 * \lg(2 * \cos^2 \varphi)$.

In practice two end angles, $\pi/2$ and $-\pi/2$, often need to be avoided, then the procedure of the normalization given by Eq. (A-6) is revised as

$$\frac{1}{\varphi_{\max} - \varphi_{\min}} \int_{\varphi_{\min}}^{\varphi_{\max}} 10^{\Delta L_W/10} d\varphi = 1, \quad (\text{A-6'})$$

with φ_{\max} being close to $\pi/2$ and φ_{\min} close to $-\pi/2$.

In addition, to avoid infinity in a numerical calculation, the dipole directivity can be approximately expressed as

$$\Delta L_{W,dipole} = 10 * \lg(0.001 + 0.999 * \cos^2 \varphi). \quad (\text{A-7'})$$

This expression gives -30 dB at the two end angles, $\pi/2$ and $-\pi/2$.

A5. A calculation procedure to determine equivalent horizontal directivity of a line source in free field ($A_{excess}(\varphi) = 0$)

For simplicity, each wagon of a train, not each wheelset, is modelled as a source element. The quantities used in the calculation are defined as below

- N : number of wagons ($N = 2m-1$, for being convenient to find the middle of a train)
 m : the order number of the middle wagon of the train
 l_0 : The length of a wagon (assumed to be the same for all)
 φ_j : Horizontal angle in relation to the middle of a train ($\varphi_j = [-89^\circ, 89^\circ]$)
 φ_{ij} : Horizontal angle in relation to the middle of the i -th wagon
 d : Measurement distance between a receiver and track
 y_i : y -coordinate value for the middle of the i -th wagon (0 for the receiver)
 $\Delta L_w(\varphi)$: Horizontal directivity function for train pass-by noise
 $\Delta L_w'(\varphi)$: Normalized horizontal directivity function for train pass-by noise
 $\Delta L_w(\varphi_{ij})$: Horizontal directivity for the i -th wagon at angle position φ_j of the train

The restrictions on N and l_0 are just for convenience. In principle N can also be an even number and l_0 can be different for various wagons.

To derive the formulae, first, the coordinate position of the i -th wagon, y_{ij} , when the train is located at the j -th angle position, φ_j , can be written as

$$\varphi_j = \tan^{-1} \left(\frac{y_m(j)}{d} \right), \quad (\text{A-8})$$

$$y_{ij} = y_m(j) + (i-m)*l_0 = d * \tan(\varphi_j) + (i-m)*l_0. \quad (\text{A-9})$$

Second, the open angle of the i -th wagon to the receiver is given by

$$\begin{aligned} \delta\varphi_{ij} &= \tan^{-1} \left(\frac{y_{ij} + 0.5l_0}{d} \right) - \tan^{-1} \left(\frac{y_{ij} - 0.5l_0}{d} \right) \\ &= \tan^{-1} \left[\tan(\varphi_j) + (i-m+0.5)*\frac{l_0}{d} \right] - \tan^{-1} \left[\tan(\varphi_j) + (i-m-0.5)*\frac{l_0}{d} \right]. \end{aligned} \quad (\text{A-10})$$

Third, the corresponding angle position of the i -th wagon is chosen to be

$$\varphi_{ij} = \tan^{-1} \left[\frac{y_{ij} - 0.5l_0}{d} \right] + \frac{\delta\varphi_{ij}}{2}. \quad (\text{A-11})$$

As has been mentioned before, for a line of incoherent and uniformly distributed monopole sources, equal angle integration will give equal contribution to the total sound power. In other words, for a line of incoherent and uniformly distributed sources of certain directivity character, its angle integrations are in general different for each equal angle range; this difference reflects the directivity effect of the line source. Thus, we obtain the formula to calculate the equivalent horizontal directivity of train pass-by noise

$$\Delta L_w(\varphi_j) = 10 \lg \left(\sum_{i=1}^N 10^{\Delta L_w(\varphi_{ij})/10} \frac{\delta\varphi_{ij}}{\Delta\varphi_{total}^j} \right), \quad (\text{A-12})$$

where

$$\Delta\varphi_{total}^j = \sum_{i=1}^N \delta\varphi_{ij} = \tan^{-1} \left[\tan(\varphi_j) + (N - m + 0.5) * \frac{l_0}{d} \right] - \tan^{-1} \left[\tan(\varphi_j) + (0.5 - m) * \frac{l_0}{d} \right]. \quad (\text{A-13})$$

Now, let us apply Eq. (A-12) to make some example calculations. The first example is to consider that monopole directivity, $\Delta L_w(\varphi_{ij}) \equiv 0$, is assigned to all source elements. Eq. (A-12) will then give the equivalent horizontal directivity as

$$\Delta L_w(\varphi_j) = 10 \lg \left(\sum_{i=1}^N \frac{\delta\varphi_{ij}}{\Delta\varphi_{total}^j} \right) = 0. \quad (\text{A-14})$$

This result says that a line of incoherent monopoles is a monopole source, irrelevant to measurement distance.

The next two calculations of practical examples consider Swedish X2 trains. One typical combination of X2 trains consists of one locomotive and six passenger wagons, each about 24 m long. Train speed is usually between 180~200 km/h. The measurements of pass-by noise have shown that noise radiation from the locomotives is about 8 dB stronger than that from passenger wagons, due to the reasons of a larger radius of the traction wheels (1,100 mm in nominal diameter for powered wheels compared with 880 mm for trailer wheels) and a higher roughness level that traction wheels usually have [A1]. Obviously, this uneven distribution in sound power along the source line has some consequence in the equivalent horizontal directivity of the line source. In the following, one calculation assumes an even distribution of the sound power and the other takes the uneven distribution into account, i.e. sound power emitted from the locomotive is 8 dB higher than those emitted from the wagons. Three measurement distances are used: 84 m (half the train length), 168 m (the train length) and 504 m (three times the train length). The resulted H-directivities are presented in Fig. A4 (the effect of the Doppler factor on H-directivity is not included). The other assumptions used in the calculations are the following: the rail radiation has been assumed to be 2.5 dB stronger than that of the wheels'. The directivity of wheel radiation is given by Eq. (3-2) and the directivity of rail radiation is assumed to be of dipole character. The simulation function of the H-directivity for the cases that sound power is uniformly distributed is given by

$$10 \lg[0.145 + 0.245 * \cos(\varphi) + 0.61 * \cos^2(\varphi)]. \quad (\text{A-15})$$

With this simulation function as the reference, it is presented in Fig. A4 how the H-directivity of the train passing-by noise varies with distance.

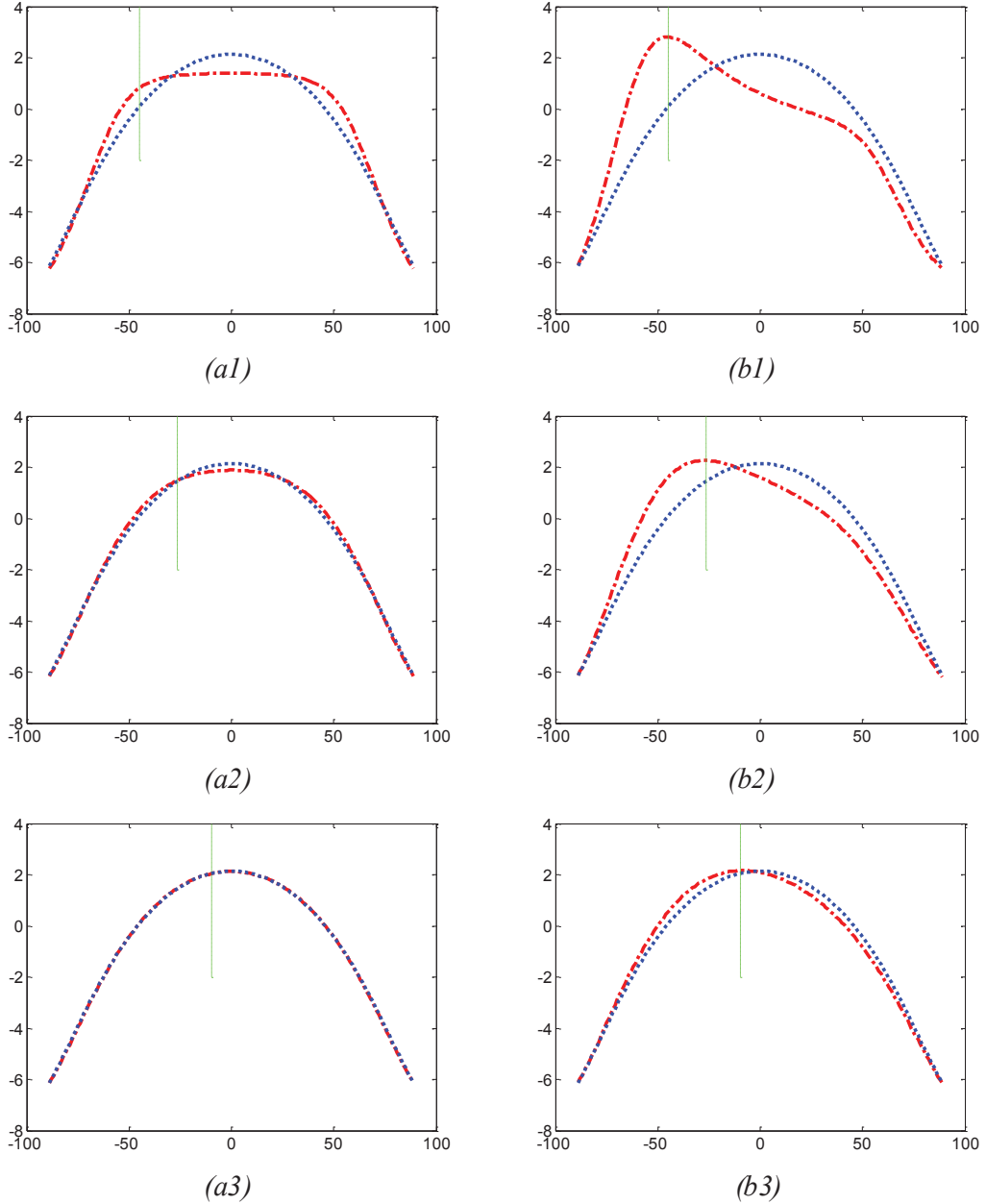


Fig. A4. Horizontal directivity of an X2 train pass-by noise. The train is $24 \times 7 = 168$ m long and moves at 180 km/h from right to left with the locomotive as the head. The measurement distance is 84 m for (a1) and (b1), 168 m for (a2) and (b2), and 504 m for (a3) and (b3). In (a1)-(a3) the sound power, or, the total roughness level, is uniformly distributed along the train while in (b1)-(b3) the sound power emitted from the locomotive is 8 dB stronger than those emitted from the wagons. Rail radiation is of dipole directivity and about 2.5 dB stronger than the wheels'; wheel radiation is of a directivity given by Eq. (3-2). For each plotting the red curve is calculated horizontal directivity using Eq. (A-12), with or without uneven distribution of the sound power considered. The blue curve is given by Eq. (A-15). The green line shows the angle position of the middle of the train when the locomotive is in front of the receiver (PS: the horizontal angle is defined in relation to the middle of the train). The effect of the Doppler factor is neglected.

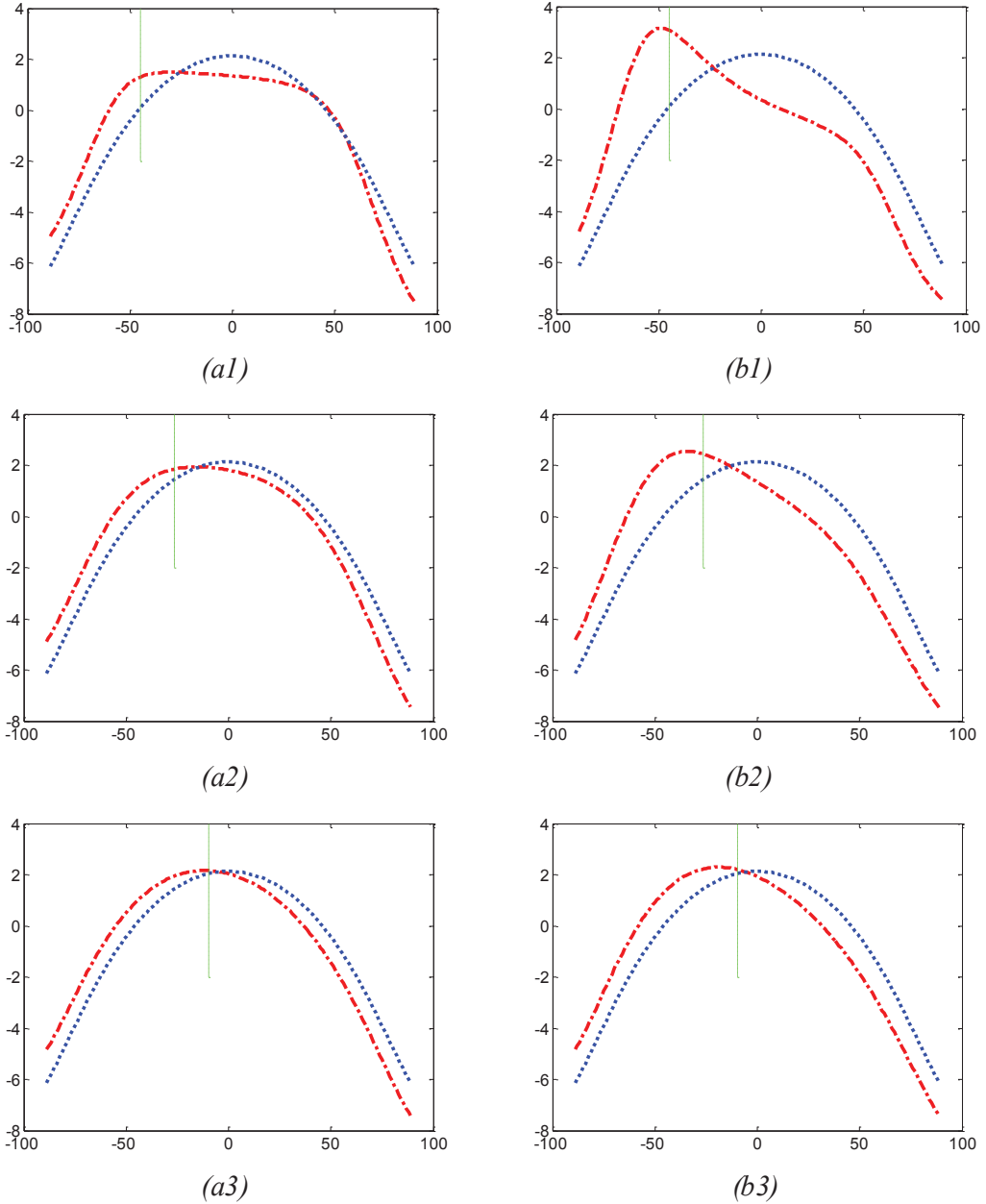


Fig. A5. Horizontal directivity of an X2 train pass-by noise. The key is the same as that in Fig. A4 while the effect of the Doppler factor on horizontal directivity is included.

Moreover, in Fig. A5, similar calculations are repeated while including the effect of the Doppler factor on H-directivity. In the calculations, train speed of 180 km/h and the speed of sound of 340 m/s are used.

According to these calculations, it can be concluded that the horizontal directivity of a line source varies with measurement distance when this distance is shorter than three times the source dimension, see (b2) and (b3) in Fig. A4. Only in cases where the sound power is approximately uniformly distributed along the source line, this distance can be relaxed to about the source dimension, see (a2) in Fig. A4. Since, as we know, the sound power distribution along a train varies from one train type to another [A1], special caution should be observed when discussing a measured horizontal directivity of train passing-by noise.

Reference

- [A1] A. Johansson, Out-of-round railway wheels – assessment of wheel tread irregularities in train traffic, *Journal of Sound and Vibration* 293 (2006) 795–806.

Annex B Calculation of Aerodynamic Noise

Calculating aerodynamic noise of flow-structure interactions usually consists of two steps: (1) to apply computational fluid dynamics (CFD) to determine the aerodynamic performance of different parts of a structure (such as pantograph, inter-coach area, door area, bogie area, etc.); (2) then, to apply computational aeroacoustics (CAA) to predict the noise.

B.1. Governing equation

The governing equation is the *Navier-Stokes* equation, which is the momentum equation for a viscous fluid and expresses the rate of change of momentum of a fluid particle in terms of pressure p , the viscous stress tensor σ_{ij} , and body forces (such as gravity) \mathbf{F} per unit volume:

$$\rho \frac{Du_i}{Dt} = F_i - \frac{\partial P_{ji}}{\partial x_j}, \quad (\text{B-1})$$

where ρ is the mass density of the flow, u the flow velocity, $\frac{D}{Dt} = \frac{\partial}{\partial t} + \vec{u} \bullet \nabla$ the convective derivative, and P_{ji} the compressive stress tensor which is given by

$$P_{ji} = p\delta_{ji} - \sigma_{ji}. \quad (\text{B-2})$$

where δ_{ji} is the Kronecker delta function. For an isotropic, *Newtonian* fluid (σ_{ij} is linear; dry air and water are two examples of such fluid) the viscous stress tensor σ becomes,

$$\sigma_{ij} = 2\eta e_{ij} + \left(\eta' - \frac{2}{3}\eta \right) \delta_{ij} e_{kk}, \quad (\text{B-3})$$

where

$$e_{ij} = \frac{1}{2} \left(\frac{\partial u_i}{\partial x_j} + \frac{\partial u_j}{\partial x_i} \right) \quad (\text{B-4})$$

is the rate of strain tensor, η and η' the shear and bulk coefficients of viscosity, respectively. These coefficients are functions of the pressure and temperature and in general vary throughout the flow, although in many cases the variations are sufficiently small that they can be neglected [56].

The bulk coefficient of viscosity η' vanishes for monatomic gases, and in this case (also for most liquids, such as water), the fluid is said to be Stokesian and with

$$\sigma_{ij} = 2\eta \left(e_{ij} - \frac{1}{3} e_{kk} \delta_{ij} \right). \quad (\text{B-5})$$

Stokes' hypothesis that the fluid is in local thermodynamic equilibrium may partially fail at high frequencies resulting a dissipation related to volume changes $\nabla \bullet \vec{u}$ which is described with a volume viscosity parameter not simply related to η .

Eq. (B-1) is a set of coupled, non-linear partial differential equations. The non-linearity is not only due to the convection term but also to turbulence which introduces additional non-linearity. Thus, it is impossible to solve these equations analytically for most engineering problems. This is the reason why CFD is attractive because it can obtain approximate computer-based solutions to the governing equations for a variety of engineering problems. However, complex flow simulations are challenging and error-prone; it takes a lot of engineering expertise to obtain validated solutions.

For a turbulent flow field, the approaches to solving the flow equations can roughly be divided into two classes. Direct numerical simulations (DNS) are extremely expensive to run because it requires huge memories. The alternative to DNS found in most CFD packages is to solve the Reynolds Averaged Navier Stokes (RANS) equations. RANS equations govern the *mean velocity and pressure* which vary smoothly in space and time making it easier to solve. However, this approach requires turbulence modelling to “close” the equations and a model of turbulence can introduce significant error into the calculation.

The $k - \varepsilon$ family of models for turbulence forms the basis of most CFD packages. Where, the Reynolds stress is modelled in terms of two turbulence parameters, the turbulent kinetic energy k and the turbulent energy dissipation rate ε , as defined below

$$k \equiv \frac{1}{2} \left(\overline{u'^2} + \overline{v'^2} + \overline{w'^2} \right) \quad (\text{B-6})$$

$$\varepsilon \equiv \nu \sum_{i=1}^3 \left[\left(\frac{\partial u'}{\partial x_i} \right)^2 + \left(\frac{\partial v'}{\partial x_i} \right)^2 + \left(\frac{\partial w'}{\partial x_i} \right)^2 \right] \quad (\text{B-7})$$

where (u', v', w') is the fluctuating velocity vector; $\nu = \mu / \rho$ the kinematic viscosity. The turbulent kinetic energy is zero for laminar flow and can be as large as 5% of the kinetic energy of the mean flow in a highly turbulent case.

(Section B.1 is mainly based on Ref. [B1].)

B.2. Acoustic calculation

Computational aeroacoustics (CAA) represents any kind of numerical method describing the noise radiation from an aeroacoustic source or the propagation of sound waves in an inhomogeneous flow field. Acoustical sources can be calculated using the flow field which is obtained by the CFD calculations. Acoustic propagation can be calculated using different methods such as Lighthill's analogy (for the sound produced by a turbulent fluid), Kirchhoff integral, Ffowcs-Williams and Hawking (FW-H) integral, Linearized Euler Equations (LEE), Expansion about Incompressible Flow (EIF), and Acoustic Perturbation Equations (APE).

The aeroacoustic sound of moving bodies, when the surface is impenetrable, is given by the FW-H integral [B2],

$$4\pi c^2 H \rho'(\vec{x}, t) = \frac{\partial^2}{\partial x_i \partial x_j} \int_V \frac{J T_{ij}}{r|1 - M_r|} d^3 \vec{\eta} - \frac{\partial}{\partial x_i} \int_S \frac{P_{ij} n_j K}{r|1 - M_r|} dS(\vec{\eta}) + \frac{\partial}{\partial t} \int_S \frac{\rho_0 \vec{v} \bullet \vec{n} K}{r|1 - M_r|} dS(\vec{\eta}), \quad (\text{B-8})$$

where H is for the Heaviside function and T_{ij} Lighthill's quadrupole source

$$T_{ij} = \rho v_i v_j + P_{ij} - c^2 (\rho - \rho_0) \delta_{ij}. \quad (\text{B-9})$$

Moreover, $\vec{\eta}$ is the moving co-ordinate system in which the sources are at rest. J is the ratio of the volume elements of the sources in the \vec{y} (in which the receiver is at rest) and $\vec{\eta}$ spaces; K is the ratio of the area elements of the surface S in the \vec{y} and $\vec{\eta}$ spaces. If all the source elements move with the same linear or angular velocity, there is no change in the area or volume occupied by the elements in $\vec{\eta}$ -space compared with in \vec{y} -space, then $J = K = 1$.

In addition, for the RHS of Eq. (B-8), the first term describes the turbulence contribution, the second term is for solid wall vibration, and the third term is due to the motion of the solid object(s).

Reference

[B1] Rajesh Bhasharan and Lance Collins, Introduction to CFD Basics,
<http://courses.cit.cornell.edu/fluent/cfd/intro.pdf>

[B2] A.P. Dowling and J.E. Ffowcs Williams, Sound and Sources of Sound, Ellis Horwood Limited 1983.

Bibliography

- [1] Wolfgang Kropp, Tor Kihlman, Jens Forssén and Lars Ivarsson, Reduction Potential of Road Traffic Noise – A Pilot Study, Applied Acoustics, Chalmers University of Technology, February 2007.
- [2] COM (2000) 468 final, Directive of the European Parliament and of the Council – relating to the Assessment and Management of Environment Noise.
- [3] European Environment Agency, TERM 2001, Indicators tracking transport and environment integration in the European Union, Copenhagen, 2001.
- [4] David Thompson, Railway Noise and Vibration: Mechanisms, Modelling and Means of Control, Elsevier 2009.
- [5] Paul J. Remington, Wheel/rail noise, I: Characterization of the wheel/rail dynamic system, *Journal of Sound and Vibration* 46 (1976) 359–379.
- [6] M. J. Rudo, Wheel/rail noise – part II: Wheel squeal, *Journal of Sound and Vibration* 46 (1976) 381–394.
- [7] I. L. Vér, C. S. Ventres and M. M. Myles, Wheel/rail noise – part III: Impact noise generation by wheel and rail discontinuities, *Journal of Sound and Vibration* 46 (1976) 395–417.
- [8] Paul J. Remington, Wheel/rail noise – part IV: rolling noise, *Journal of Sound and Vibration* 46 (1976) 419–436.
- [9] A. G. Galaitis and E. K. Bender, Wheel/rail noise – part V: Measurement of wheel and rail roughness, *Journal of Sound and Vibration* 46 (1976) 437–451.
- [10] D. J. Thompson, Wheel-rail noise: theoretical modelling of the generation of vibration, PhD thesis, University of Southampton (1990).
- [11] H. Mahé, D. J. Thompson, A. Zach, G. Hödl, Experimental validation of the prediction model TWINS for rolling noise, pp. 1459–1462, *Proceedings of inter.noise93*, 24-26 August, Leuven, Belgium.
- [12] D. J. Thompson and P. E. Gautier, TWINS: A prediction model for wheel-rail rolling noise, pp. 1463–1466, *Proceedings of inter.noise93*, 24-26 August, Leuven, Belgium.
- [13] About MetaRail project: <http://cordis.europa.eu/transport/src/metarail.htm>
- [14] About STAIRRS project: <http://www.stairrs.org/>

- [15] About the projects of Silent Freight, Silent Track, and Eurosabot:
<http://ec.europa.eu/research/growth/gcc/projects/in-action-rail.html>
- [16] About the projects of Harmonoise and Imagine: <http://www.imagine-project.org/artikel.php?ac=direct&id=289>
- [17] About NOEMIE project: Noise Emission Measurement Campaign for High-Speed Interoperability in Europe. See: Fodiman, P., Project NOEMIE final Report (Project n° 2002/EU/1663), July, 2005.
- [18] P. Fodiman, NOise Emission Measurement campaign for high-speed Interoperability in Europe: the NOEMIE Project, Euronoise2003, 19-21 May, Naples, Italy.
- [19] Final International Seminar, The results of the Dutch Noise Innovation Programme – Railways (IPG-Rail), Doorn, The Netherlands, 9 December , 2008.
- [20] WG Railway Noise of the European Commission, Position Paper on the European strategies and priorities for railway noise abatement, 2003.
- [21] <http://en.wikipedia.org/wiki/Shinkansen>
- [22] <http://en.wikipedia.org/wiki/TGV>
- [23] <http://en.wikipedia.org/wiki/Intercity-Express>
- [24] http://en.wikipedia.org/wiki/ETR_500
- [25] <http://en.wikipedia.org/wiki/AVE>
- [26] http://en.wikipedia.org/wiki/Korea_Train_Express
- [27] http://en.wikipedia.org/wiki/High-speed_rail_in_China
- [28] http://en.wikipedia.org/wiki/Taiwan_High_Speed_Rail
- [29] C. Mellet, F. Létourneau, F. Poisson and C. Tallote, High Speed Train Noise Emission: Latest investigation of the aerodynamic/rolling noise contribution, *Journal of Sound and Vibration* 293 (2006) 986–994.
- [30] C. Charbonnel, Definition of a simple model of sources for the TGV-R, *HAR12TR-021206-SNCF01* (the Harmonoise technical report).
- [31] F. Poisson, P.E. Gautier and F. Letourneau, Noise Sources for High Speed Trains: A Review of Results in the TGV Case, Noise and Vibration Mitigation for Rail Transportation Systems, *Notes on Numerical Fluid Mechanics and Multidisciplinary Design*, Volume 99, ©2008 Springer-Verlag Berlin Heidelberg.
- [32] W.F. King III, A précis of developments in the aeroacoustics of fast trains, *Journal of Sound and Vibration* 193 (1996) 349-358.
- [33] C. Talote, P.E. Gautier, D.J. Thompson, C. Hanson, Identification, modelling and reduction potential of railway noise sources: a critical survey, *Journal of Sound and Vibration* 267 (2003) 447-468.

- [34] B. S. Holmes, J. B. Dias, B. A. Jaroux, T. Sassa and Y. Ban, Predicting the wind noise from the pantograph cover of a train, *International Journal for Numerical Methods in Fluids*, vol. 24, 1307-1319 (1997).
- [35] T. Sassa, T. Sato and S. Yatsui, Numerical analysis of aerodynamic noise radiation from a high-speed train surface, *Journal of Sound and Vibration* 247 (2001) 407-416 .
- [36] X. Golerfelt, C. Bailly and D. Juvé, Direct computation of the noise radiated by a subsonic cavity flow and application of integral methods, *Journal of Sound and Vibration* 266 (2003) 119-146.
- [37] F. Mizushima, C. Kato, T. Kurita and A. Lida, Investigation of aerodynamic noise generated from a train car gap, *Proceedings of Inter Noise 2006*, Honolulu, Hawaii (USA), 3-6 December.
- [38] Paul Nelson, Transportation Noise, Reference Book, Butterworth & Co. Ltd., 1987.
- [39] S. Peters, The Prediction of Railway Noise Profiles, *Journal of Sound and Vibration* 32 (1974) 87-99.
- [40] X. Zhang, Measurements of Directivity on Test Rig, *HAR12TR-020910-SP04*, 30 April, 2003 (the Harmonoise technical report).
- [41] X. Zhang and H. Jonasson, Directivity of Railway Noise Sources, *Journal of Sound and Vibration* 293 (2006) 995–1006.
- [42] Xuetao Zhang, To determine the horizontal directivity of a train pass-by, in03_627, *Proceedings of Inter Noise 2003*, Jeju (Korea), 25-28 August.
- [43] X. Zhang, Directivity of Railway Rolling Noise, Noise and Vibration Mitigation for Rail Transportation Systems, *Notes on Numerical Fluid Mechanics and Multidisciplinary Design*, Volume 99, ©2008 Springer-Verlag Berlin Heidelberg.
- [44] C.H. Chew, Vertical directivity of train noise, *Applied Acoustics* vol. 51, No. 2, pp. 157 – 168, 1997.
- [45] C.H. Chew, Vertical directivity pattern of train noise, *Applied Acoustics* vol 55, No. 3, pp. 243 – 250, 1998.
- [46] W. K. Lui, K. M. Li, C. W. M. Leung and G. M. Frommer, An experimental study of the vertical directivity pattern of wheel/rail rolling noise, *Acta Acustica united with Acustica*, Vol. 93 (2007) 742-749.
- [47] T. Ten Wolde and C. J. M. van Ruiten, Sources and mechanisms of wheel/rail noise: state-of-art and recent research, *Journal of Sound and Vibration* 87 (1983) 147-160.
- [48] D. J. Thompson and C. J. C. Jones, Sound radiation from a vibrating railway wheel, *Journal of Sound and Vibration* 253 (2002) 401-419.
- [49] D. J. Thompson, C. J. C. Jones and N. Turner, Investigation into the validity of two-dimensional models for sound radiation from waves in rails, *Journal of Acoustical Society of America* 113 (2003) 1965-1974.

- [50] T. Kitagawa and D. J. Thompson, The horizontal directivity of noise radiated by a rail and implications for the use of microphone arrays, *Journal of Sound and Vibration* 329 (2010) 202-220.
- [51] X. Zhang, Railway Traction Noise – the state of the art, *HAR12TR-030530-SP01* (the Harmonoise technical report).
- [52] C. Czolbe and M. Hecht, Noise reduction measures at freight train locomotives “Blue Tiger”, Noise and Vibration Mitigation for Rail Transportation Systems, *Notes on Numerical Fluid Mechanics and Multidisciplinary Design*, Volume 99, ©2008 Springer-Verlag Berlin Heidelberg.
- [53] <http://www.charmec.chalmers.se/about/>
- [54] T.X. Wu and D.J. Thompson, A hybrid model for the noise generation due to railway wheel flats, *Journal of Sound and Vibration* 251 (2002) 115-139.
- [55] T.X. Wu and D.J. Thompson, On the impact noise generation due to a wheel passing over rail joints, *Journal of Sound and Vibration* 267 (2003) 485-496.
- [56] M.S. Howe, *Acoustics of Fluid-Structure Interactions*, Cambridge University Press 1998.
- [57] H. Matsumoto, K. Saitoh and T. Issiki, A method of reducing aerodynamic sounds generated by bent round bars in a uniform air-flow, *Proceedings of Inter Noise 2006*, Honolulu, Hawaii (USA), 3-6 December.
- [58] Christopher K. W. Tam, Intensity, spectrum, and directivity of turbulent boundary layer noise, *Journal of Acoustical Society of America* 57(1) (1975) 25-34.
- [59] S. Glegg, Fan noise, Chapter 19, *Noise and Vibration* (Edited by R. G. White & J. G. Walker, Ellis Horwood Ltd., 1982).
- [60] M. Dittrich, The IMAGINE Source Model for Railway Noise Prediction, *Acta Acustica United with Acustica* 93 (2007) 185–200.
- [61] <http://www.microflown.com/>